



**UNIVERSIDAD DE INVESTIGACIÓN DE TECNOLOGÍA  
EXPERIMENTAL YACHAY**

**Escuela de Ciencias Químicas e Ingeniería**

**Electrochemical Sensors Based on Conducting Polymers for Organic  
Molecules Detection**

Trabajo de integración curricular presentado como requisito para la  
obtención del título de Químico

**Autor:**

Francisco Alexander Bravo Plascencia

**Tutor:**

Ph.D Alex Uriel Palma Cando.

Urcuquí, septiembre de 2020

**SECRETARÍA GENERAL**  
(Vicerrectorado Académico/Cancillería)  
**ESCUELA DE CIENCIAS QUÍMICAS E INGENIERÍA**  
**CARRERA DE QUÍMICA**  
**ACTA DE DEFENSA No. UITEY-CHE-2020-00050-AD**

A los 5 días del mes de octubre de 2020, a las 15:00 horas, de manera virtual mediante videoconferencia, y ante el Tribunal Calificador, integrado por los docentes:

<u>Presidente Tribunal de Defensa</u>	<u>Dr. VILORIA VERA, DARIO ALFREDO , Ph.D.</u>
<u>Miembro No Tutor</u>	<u>Mgs. DE LIMA ELJURI, LOLA MARIA</u>
<u>Tutor</u>	<u>Dr. PALMA CANDO, ALEX URIEL , Ph.D.</u>

El(la) señor(ita) estudiante BRAVO PLASCENCIA, FRANCISCO ALEXANDER, con cédula de identidad No. 1105052649, de la ESCUELA DE CIENCIAS QUÍMICAS E INGENIERÍA, de la Carrera de QUÍMICA, aprobada por el Consejo de Educación Superior (CES), mediante Resolución RPC-SO-39-No.456-2014, realiza a través de videoconferencia, la sustentación de su trabajo de titulación denominado: ELECTROCHEMICAL SENSORS BASED ON CONDUCTING POLYMERS FOR ORGANIC MOLECULES DETECTION, previa a la obtención del título de QUÍMICO/A.

El citado trabajo de titulación, fue debidamente aprobado por el(los) docente(s):

<u>Tutor</u>	<u>Dr. PALMA CANDO, ALEX URIEL , Ph.D.</u>
--------------	--

Y recibió las observaciones de los otros miembros del Tribunal Calificador, las mismas que han sido incorporadas por el(la) estudiante.

Previamente cumplidos los requisitos legales y reglamentarios, el trabajo de titulación fue sustentado por el(la) estudiante y examinado por los miembros del Tribunal Calificador. Escuchada la sustentación del trabajo de titulación a través de videoconferencia, que integró la exposición de el(la) estudiante sobre el contenido de la misma y las preguntas formuladas por los miembros del Tribunal, se califica la sustentación del trabajo de titulación con las siguientes calificaciones:

Tipo	Docente	Calificación
Miembro Tribunal De Defensa	Mgs. DE LIMA ELJURI, LOLA MARIA	9,9
Tutor	Dr. PALMA CANDO, ALEX URIEL , Ph.D.	9,9
Presidente Tribunal De Defensa	Dr. VILORIA VERA, DARIO ALFREDO , Ph.D.	10,0

Lo que da un promedio de: 9.9 (Nueve punto Nueve), sobre 10 (diez), equivalente a: APROBADO

Para constancia de lo actuado, firman los miembros del Tribunal Calificador, el(la) estudiante y el(la) secretario ad-hoc.

*Certifico que en cumplimiento del Decreto Ejecutivo 1017 de 16 de marzo de 2020, la defensa de trabajo de titulación (o examen de grado modalidad teórico práctica) se realizó vía virtual, por lo que las firmas de los miembros del Tribunal de Defensa de Grado, constan en forma digital.*

**BRAVO PLASCENCIA, FRANCISCO ALEXANDER**  
Estudiante

Dr. VILORIA VERA, DARIO ALFREDO , Ph.D.  
Presidente Tribunal de Defensa

DARIO ALFREDO VILORIA VERA  
Firmado digitalmente por DARIO ALFREDO VILORIA VERA  
Fecha: 2020.10.06 08:52:35 -05'00'

Dr. PALMA CANDO, ALEX URIEL , Ph.D.  
Tutor

 Firmado digitalmente por ALEX URIEL PALMA CANDO

Mgs. DE LIMA ELJURI, LOLA MARIA  
Miembro No Tutor

LOLA MARIA DE LIMA ELJURI  
Digitally signed by  
LOLA MARIA DE LIMA  
ELJURI  
Date: 2020.10.05  
20:32:21 -05'00'

CIFUENTES TAFUR, EVELYN CAROLINA  
Secretario Ad-hoc



firmado digitalmente por:  
EVELYN CAROLINA  
CIFUENTES TAFUR

## AUTORÍA

Yo, Francisco Alexander Bravo Plascencia, con cédula de identidad 1105052649, declaro que las ideas, juicios, valoraciones, interpretaciones, consultas bibliográficas, definiciones y conceptualizaciones expuestas en el presente trabajo; así cómo, los procedimientos y herramientas utilizadas en la investigación, son de absoluta responsabilidad de el/la autora(a) del trabajo de integración curricular. Así mismo, me acojo a los reglamentos internos de la Universidad de Investigación de Tecnología Experimental Yachay.

Urcuquí, septiembre de 2020.

A handwritten signature in blue ink, appearing to read 'Francisco Bravo', written over a horizontal line.

Francisco Bravo

CI: 1105052649

## AUTORIZACIÓN DE PUBLICACIÓN

Yo, Francisco Alexander Bravo Plascencia, con cédula de identidad 1105052649, cedo a la Universidad de Tecnología Experimental Yachay, los derechos de publicación de la presente obra, sin que deba haber un reconocimiento económico por este concepto. Declaro además que el texto del presente trabajo de titulación no podrá ser cedido a ninguna empresa editorial para su publicación u otros fines, sin contar previamente con la autorización escrita de la Universidad.

Asimismo, autorizo a la Universidad que realice la digitalización y publicación de este trabajo de integración curricular en el repositorio virtual, de conformidad a lo dispuesto en el Art. 144 de la Ley Orgánica de Educación Superior.

Urququí, septiembre de 2020.

A handwritten signature in blue ink, appearing to read 'Francisco Bravo', written over a horizontal line.

Francisco Bravo

CI: 1105052649

*To my brothers Augusto, Vladimir, Cesar, Andres, Cristian and Carlos and also to my parents Cesar and Carmen for their unconditional support that allow me to be in this moment. Besides, I would like to dedicate this work to my grandfather who believe in me since I was a child.*

## **Acknowledgments**

Thanks to good, for giving me tenacity and patience to see my goals fulfilled. Then, I fully thank my parents for advise me, support me and motivate me in the most difficult moment of my carrier. Additionally, I want to thank to my brothers who were always there for me despite the distance.

Furthermore, I would like to express gratitude to the members of department H1-4 for be like my bothers in the university and for more than 3 years of amazing experiences. Additionally, I want say thanks my friends from fist semesters and carrier and to my teachers of Yachay Tech for their daily effort to give me a comprehensive and high-level training and for having taught me to love science.

Thanks to my research partner, Alvaro Terán, who worked with me shoulder to shoulder in different projects related to this thesis. I want to also thank the members of jury MSc. Lola De Lima and Dr. Alfredo Viloría for reviewing this research work. Finally, I would like to give special thanks to my tutor, Dr. Alex Palma Cando how despite the situation that the world is going through, he continued motivating me and guiding the realization of this work.

## Resumen

Moléculas orgánicas como los neurotransmisores y el ácido úrico tienen un papel fundamental en la regulación del funcionamiento del cuerpo humano. Por lo cual, la detección y cuantificación de esas moléculas en fluidos humanos tienen una relevancia farmacéutica y terapéutica. En ese contexto, los sensores electroquímicos aparecen como una opción de aplicación in situ, rápida, fácil de usar y de bajo costo para la determinación de moléculas orgánicas en solución. Los polímeros conductores (CPs) son materiales muy explorados en la fabricación de sensores debido a su alta conductividad eléctrica, versatilidad, múltiples vías de síntesis y estabilidad en condiciones ambientales. Este documento es una revisión bibliográfica actualizada de los trabajos de investigación más relevantes sobre sensores electroquímicos basados en polímeros conductores y su aplicación en la determinación de dopamina, epinefrina, serotonina y ácido úrico. Se realizó un análisis del proceso de síntesis y caracterización morfológica destacando los diferentes tipos de micro y nano estructuras, generadas para el polímero por sí mismo o la combinación de diferentes materiales en un compuesto. Además, se comparó el rendimiento y la capacidad de los sensores a base de CPs para detectar trazas de las moléculas orgánicas previamente mencionadas. Estos análisis se realizaron utilizando como parámetro la sensibilidad y el límite de detección (LOD) y también se evaluó como afectan la mesoporosidad, microporosidad y rugosidad de la superficie del electrodo a las estas figuras de mérito. Esta revisión bibliográfica considera las publicaciones científicas realizadas desde 2015 a 2020; donde el polipirrol (PPy), polianilina (PANI) y poli (3,4-etilendioxitiofeno (PEDOT) figuran como los CPs más utilizados para la construcción de sensores electroquímicos.

**Palabras clave:** Neurotransmisores, dopamina, epinefrina, serotonina, ácido úrico, polímeros conductores, sensores electroquímicos, límite de detección (LOD)

## Abstract

Organic molecules such as neurotransmitters and uric acid have a fundamental role in the human body function regulation. Therefore, the detection and quantification of those molecules in human fluid have a pharmaceutical and therapeutically relevance. In that context, the electrochemical sensors appear as a low cost, rapid, easy to use and in situ application option for determination of organic molecules in liquid solution. Conducting polymers (CPs) are very explored sensor building materials because its high electrical conductivity, versatility, multiple synthesis pathways and stability in environmental conditions. This document presents a state-of-the-art review of the most relevant research about electrochemical sensors based on conducting polymers and their application in the determination of dopamine, epinephrine, serotonin and uric acid. An analysis of the synthetic process and morphological characterization was carried out, highlighting the different types of micro and nano structures, generated for the polymer itself or the combination with different materials in a composite. Furthermore, the performance and ability to detect traces of previous mentioned molecules by CPs based sensors is compared. These analyzes were performed using the sensitivity and the limit of detection (LOD) as parameters, and it was also evaluated how the mesoporosity, microporosity and roughness of the electrode surface affect these figures of merit. This bibliographic review considers the scientific publications made from 2015 to 2020; where polypyrrole (PPy), polyaniline (PANI) and poly (3,4-ethylenedioxythiophene (PEDOT) appear as the most recurrent CPs for the construction of electrochemical sensors.

**Keywords:** Neurotransmitters, dopamine, epinephrine, serotonin, uric acid, conducting polymers, electrochemical sensor, limit of detection (LOD)

## ABBREVIATIONS AND ACRONYMS

<b>µm</b>	Micro Molar
<b>3-TBA</b>	3-Thiophene boronic acid
<b>afGQDs</b>	Amino-functionalized graphene quantum dots
<b>AFM</b>	Atomic force microscopy
<b>AGCE</b>	Anodized glassy carbon electrode
<b>AHMP</b>	Poly-4-Amino-6-hydroxy-2-mercaptopyrimidine
<b>APS</b>	Ammonium persulphate
<b>BSA</b>	Bovine serum albumin
<b>C#</b>	Carbon- coated mesoporous
<b>CD</b>	Cyclic dextrin
<b>CE</b>	Counter electrode
<b>CNT</b>	Carbon nanotubes
<b>CP</b>	Conducting polymers
<b>CPE</b>	Carbon paste electrode
<b>CV</b>	Cyclic voltammetry
<b>DA</b>	Dopamine
<b>DMF</b>	N,N-Dimethylmethanamide
<b>DPV</b>	Differential pulse voltammetry
<b>E</b>	Voltage
<b>EB</b>	Electron Beam
<b>EBT</b>	Eriochrome black T
<b>EDOT</b>	(3,4-ethylenedioxythiophene)
<b>EP</b>	Epinephrine
<b>ERGO</b>	Electrochemical reduced graphene oxide
<b>FA</b>	Poly-fuchsine acid
<b>FESEM</b>	Field emission scanning electron microscopy
<b>f-MWCNTs</b>	Functionalized multi-walled carbon nanotubes
<b>FTIR</b>	Fourier- transformed infrared spectroscopy
<b>FTO</b>	Fluoride thin oxide
<b>GCE</b>	Glassy carbon electrode
<b>GO</b>	Graphene oxide
<b>GP</b>	Graphene
<b>HXA</b>	Hypoxanthine
<b>i</b>	Current
<b>IL</b>	Ionic liquid
<b>ITO</b>	Indium thin oxide
<b>IUPAC</b>	International Union of Pure and Applied chemistry
<b>LOD</b>	Limit of detection
<b>LSG</b>	Laser scribed graphene
<b>LSV</b>	Linear swipe voltammetry
<b>MIP</b>	Molecular imprinted polymers
<b>MOF</b>	Metal- organic framework
<b>MS</b>	Mass spectroscopy

<b>ms</b>	millisecond
<b>mV</b>	millivolts
<b>MWCNT</b>	Multi Wall carbon nanotubes
<b>Nf</b>	Nano fiber
<b>NPs</b>	Nanoparticles
<b>OPPy</b>	Overoxidized electropolymerized polypyrrole
<b>p(P3CA)</b>	Poly(pyrrole-3-carboxylic acid)
<b>P3-TBA</b>	Poly 3-Thiophene boronic acid
<b>P6-TG</b>	Poly(6-thioguanine)
<b>p-AHNSA</b>	Poly 4-amino-3-hydroxy-1-naphthalenesulfonic acid
<b>PAMT</b>	Poly (2-amino-5-mercapto-1, 3, 4-thiadiazole)
<b>PANI</b>	Polyaniline
<b>PANI-co-PoAN</b>	Poly(aniline-co-o-anisidine)
<b>PAPBA</b>	Poly (3-aminophenylboronic acid)
<b>PBCB</b>	Poly (brilliant cresyl blue)
<b>PBS</b>	Phosphate buffer solution
<b>PDNs</b>	Polydopamine nanospheres
<b>pEBT</b>	Poly (eriochrome black T)
<b>PEDOT</b>	Poly(3,4-ethylenedioxythiophene)
<b>PEDOT:PSS</b>	Poli(3,4-etilendioxitiofeno)-poli(estireno sulfonato)
<b>PGBHA</b>	Poly(glyoxal-bis(2-hydro- xyanil)
<b>pHQ</b>	Poly (hydroquinone)
<b>PNEDA</b>	Poly(N-( Naphthyl) ethylenediamine dihydrochloride)
<b>Poly(BCG)</b>	Poly (bromocresol green)
<b>poly(p-ABSA)</b>	Poly (p-amino benzene sulfonic acid)
<b>Poly(TB)</b>	Polytoluidine blue
<b>poly-TrB</b>	Poly-Trypan Blue
<b>POMA</b>	Poly (o-methoxyaniline)
<b>p-ProH</b>	Poly (procatamol hydrochloride)
<b>PPy</b>	Polyporrrole
<b>Pr</b>	Poly(3,4-ethylenedioxythiophene)
<b>PS</b>	Polysudan III
<b>PSA</b>	Poly(sulfosalicylic acid)
<b>p-TPP</b>	Polytetraphenylporphyrin
<b>pTSA</b>	p-toluene sulphonic acids
<b>PVP</b>	Polyvinylpyrrolidone
<b>RE</b>	Reference electrode
<b>rGo</b>	Reduced graphene oxide
<b>SDS</b>	Sodium dodecyl sulfate
<b>SEM</b>	Scanning electron microscopy
<b>SER</b>	Serotonin
<b>SPCs</b>	Screen printed carbon sensor
<b>SWV</b>	Square wave voltammetry
<b>SβCD</b>	Sulfonated β-cyclodextrin

<b>TEM</b>	Transmission electron microscopy
<b>UA</b>	Uric acid
<b>WAXD</b>	Wide angle X-Ray diffraction
<b>WE</b>	Working electrode
<b>XA</b>	Xanthine
<b>ZNRs</b>	Zinc Nano rods
<b>ZNTs</b>	Zinc nanotubes

## INDEX

<b>AUTORÍA</b> .....	ii
<b>AUTORIZACIÓN DE PUBLICACIÓN</b> .....	iii
<b>Acknowledgments</b> .....	v
<b>Resumen</b> .....	vi
<b>Abstract</b> .....	vii
<b>ABREVIATIONS AND ACRONYMS</b> .....	viii
<b>INDEX</b> .....	xi
<b>INTRODUCTION</b> .....	1
<b>1.1 General introduction</b> .....	1
<b>1.2 Fundamentals of the Electrochemical Sensors</b> .....	2
<b>1.3 Fundamentals of the figures of merit</b> .....	4
<b>1.4 Conduction polymer sensors mechanism of detection</b> .....	5
<b>1.5 Problem statement</b> .....	6
<b>1.6 General and specific objectives</b> .....	7
<b>STATE-OF-THE-ART REVIEW</b> .....	8
<b>2.1 Dopamine</b> .....	8
<b>2.2 Ephinefrine</b> .....	24
<b>2.3 Serotonin</b> .....	29
<b>2.4 Uric Acid</b> .....	33
<b>CONCLUSIONS</b> .....	38
<b>RECOMMENDATIONS</b> .....	38
<b>REFERENCES</b> .....	40

## INTRODUCTION

### 1.1 General introduction

Neurotransmitter are molecules responsible to transmit the neurological signal and permit the intercellular communication between neuron cells<sup>1,2</sup>. The body concentration of these molecules affects the brain work, frame of mind, pain response and physical performance<sup>3</sup>. Besides, they regulate the process of consciousness, motivation and memorization<sup>4</sup>. It means that correct balance of neurotransmitters concentration in body is fundamental to maintain the human health, and prevent disease and mental disorders<sup>2</sup>. Based on these facts, the determination and quantification of the concentration of neurotransmitters in human fluids is critical towards a better and fast diagnostic and treatment of different diseases and disorders. On the other hand, Uric Acid (AU) appear as a very important biomarker because it is a final product purine metabolism and it is easily accumulated in the human body do to its solubility. The high or low concentration of UA is a signal of metabolic alterations or disease appearance<sup>5,6</sup> and for that reason it is very important to quantification of this organic molecule in human fluids.

Many techniques had been developed for sensing and quantification of organic molecules in solution. One of the most used technique is colorimetry by the employing of different nanostructured materials in order to improve the sensitivity of method<sup>7-12</sup> a chemical reaction with the analyte<sup>13,14</sup>. Fluorometry appears as a technique with high performance for this type of sensing which include the use of quantum dots<sup>15,16</sup> nanostructured materials<sup>6,17-19</sup> and chemical reagent<sup>20,21</sup>. In addition, mass spectroscopy (MS) coupled to Liquid chromatography for neurotransmitter and Uric acid (UA) quantification had been reported<sup>22-26</sup>. Those research works shown a different and specialized kind of MS technique such as isotope dilution MS<sup>5</sup> high-resolution Orbitrap<sup>27</sup> and with polarity switching electrospray<sup>28</sup>, Photoelectrochemical<sup>29</sup>, Photoluminescence<sup>30</sup>, Chemiluminescence<sup>31</sup>, Electronic<sup>32</sup> and Chemical methods<sup>33</sup> based sensor has also been used. On the other hand, electrochemical sensors appear as a powerful method for detection of organic molecules in solution. This method is based on the redox reaction and electrochemical activity of sensor surface and analyte<sup>34</sup>. It presents many advantages in comparison with other techniques. The most relevant ones are the high accuracy, notably high sensitivity, excellent selectivity and demonstrated reproducibility<sup>35,36</sup>. In addition, this type of sensors has low cost of production and easy miniaturization because the simplicity of equipment required for performance this technique<sup>37,38</sup>. A fast response, real time monitoring, in situ detection and green behavior<sup>39-42</sup>, contribute to positions the

electrochemical detection method as one of the greatest potential technique in the field of sensing of molecules in solution and its used in environmental and health science.

Currently, a huge variety of materials had been employed for build electrochemical sensor with the aim of improve certain characteristics such as electrical conductivity, surface area, stability and both mechanical and chemical stability<sup>43</sup>. Besides, the building material selection pretend to solve some problems of electrochemical sensors as electrode fouling and overlapping of oxidant potential of molecules presented a sample<sup>44</sup>. In that context, conducting polymers (CPs) appears like one of the most relevant and used materials for molecules sensing by their unique physical and chemical properties which variate by the length of conjugation and overall chain<sup>45,46</sup>. Additionally, CPs had application in the field of supercapacitors, batteries, solar cell, electrochromic and clearly in electrochemical sensors<sup>46,47</sup>. CPs, as electrochemical materials, present special characteristic including relatively high electrical conductivity, ease of being affected by external molecules, adjustable architecture, adaptability, versatility, room stability and sensitive to surfer changes in its electrochemical activity with tiny changes in its surface<sup>47-49</sup>.

## **1.2 Fundamentals of the Electrochemical Sensors**

The electrochemical sensor, including CP based sensors, required for its performance to occupy an electrochemical cell which is controlled by a potentiostat and made up by three kind of electrodes<sup>50</sup>. The first one is the working electrode (WE) which accomplish the event of study. The second one corresponds to reference electrode (RE) that is a semi cell with well-defined and stable equilibrium potential and helps to control the potential applied to WE. And finally, the third one is the counter electrode (CE) have the function of close the circuit and be the surface where the complementary semi -redox reaction occurs. Besides, the electrochemical cell employs a solution called supporting electrolyte that is a molecule that do not reacts in the same potential than analyte and improve the conductivity<sup>51</sup>. This mentioned set up allows to perform techniques using and controlling the potential (E) like excitation stimulus in order to obtain current (i) as response signal as Ohms law postulate ( $E = R \times i$ )<sup>50</sup>. The more used potentiodynamic techniques are cyclic voltammetry (CV), differential pulse voltammetry (DPV), square wave voltammetry (SWV), and linear sweep voltammetry (LSV). Figure 1 shows the excitation stimulus (a) and repose (b) of CV which requires a triangular scan from initial E to final E a then back to initial E to generate a response signal current corresponding to oxidation and reduction of analyte<sup>51</sup>. In the case of LSV the scan of E goes in one direction

from  $E_0$  to  $E_1$  as shows Figure 2. The obtained current signal is produced by just one semi – redox reaction <sup>50</sup>.

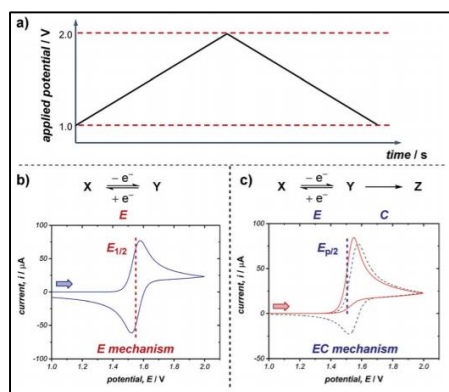


Figure 1: a)Excitation stimulus of CV and b) response of both semi redox reaction of CV.

Adopted from <sup>52</sup>

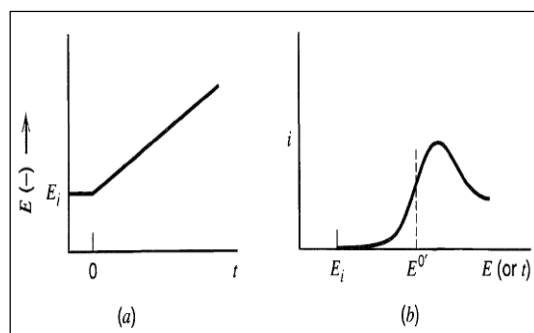


Figure 2: a)Excitation stimulus of LSV and b) response of semi redox reaction of LSV.

Adopted from <sup>50</sup>

DPV and SWV are similar techniques using a pulse of E to obtain more resolute current signals by the differentiation between Faraday current (redox reaction) and non-Faradaic current (double layer) <sup>50</sup>. This characteristic improves the sensibility of method and became this technique perfect for traces detection <sup>53</sup>. Figure 3 show the applied potential profile used in DPV which consist in small potential pulse with amplitude of 1mv - 100 mv applied in periods of 10 ms to 100 ms <sup>54</sup>. Those pulses are overlapped to a normal LSV <sup>53</sup> and for reason the current is measured in the point  $i_1$  and  $i_2$  <sup>54</sup>.The obtained voltammograms is the plot of difference of mentioned currents vs the applied E <sup>53</sup>.

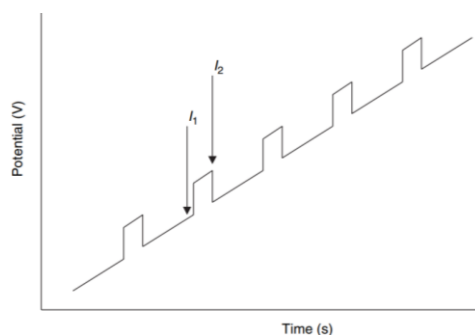


Figure 3: Excitation stimulus profile of DPV. Adopted from <sup>54</sup>

SWV is very similar to DPV but they differ mainly in the shape of the pulse used as is possible to observe in Figure 3 and Figure 4. SWV excitation stimulus shows a voltage increasing profile made of two parts: the first one is a LSV coupled to a square voltage pulse in a period corresponding to the length of wave as Figure 4 shows <sup>55</sup>. The voltammograms are built with the differences between  $i_{fwd}$  and  $i_{rev}$  vs the applied potential <sup>56</sup>.

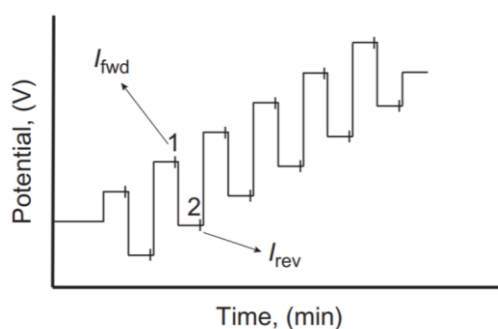


Figure 4: Excitation stimulus of SWV. Adopted from <sup>55</sup>

### 1.3 Fundamentals of the figures of merit

The figures of merit permit to compare different developed methods and their detecting performance<sup>57</sup>. The most relevant ones for the purposes of this work are sensitivity, linear analytical range and limit of detection (LOD). It is because the sensibility in univariate calibration is defined for the International Union of Pure and Applied Chemistry (IUPAC) as changes in response of apparatus by unit of change of analyte of inters <sup>57,58</sup>. The slope of calibration curve is used as quantitative parameter of sensitivity. It means that a method with large slope will show a huge change in response with small changes in concentration of analyte.<sup>59</sup> The concept of sensitivity just can be well defined and appreciated in a specific range of concentrations named as linear analytical range <sup>58,59</sup>. Based in that fact, the linear analytical range of methods can be establish in the concentration range where the sensibility remains constant with a defined tolerance<sup>60</sup>. In the case of LOD, an accurate description is, the minimum of analyte that can be detected with acceptable certain degree<sup>58</sup>. It means that LOD is the point

that separate the section of analyte detected but with not enough evidence to confirm its presence in the sample, and analyte detected with enough evidence. According to Justino et al.<sup>59</sup>, the LOD can be calculated using the formula,  $LOD = ks$ , where  $k$  is a factor number (3 is normally used) and  $s$  is the standard deviation of the blank. This formula assures that there is a 5% chance that signal generated by the blank be higher than  $ks$ <sup>59</sup>.

#### **1.4 Conduction polymer sensors mechanism of detection**

All reaction that occurs inside of electrochemical cell are affected by some factor that influence the electrode reaction rate and current. Those factor listed above and show in Figure 5<sup>50</sup>:

- Mass transfer
- Electron transfer at the electrode surface
- Previous and following chemical coupled reactions
- Surface reactions, such as adsorption, desorption

These factors will influence the mechanism through which the sensor and analyte interacts and for this reason the manipulation of those factors are going to determine figures of merit shown by electrochemical sensor. In that point, the flexible architecture and adaptability of CP<sup>48</sup> represent a great advantage because CP during synthesis processes or posterior generate film with different types of structures such as mesoporosity<sup>61</sup>, microporosity<sup>62</sup> or other 2d and 3d nano structures; obtaining as a result a large specific surface area which increase the electron transfer and sensibility<sup>63,64</sup>. Additionally, it is important to mention that the interaction that occurs between CP and analyte during electrochemical reaction is the electrostatic and non-covalent type<sup>48</sup>.

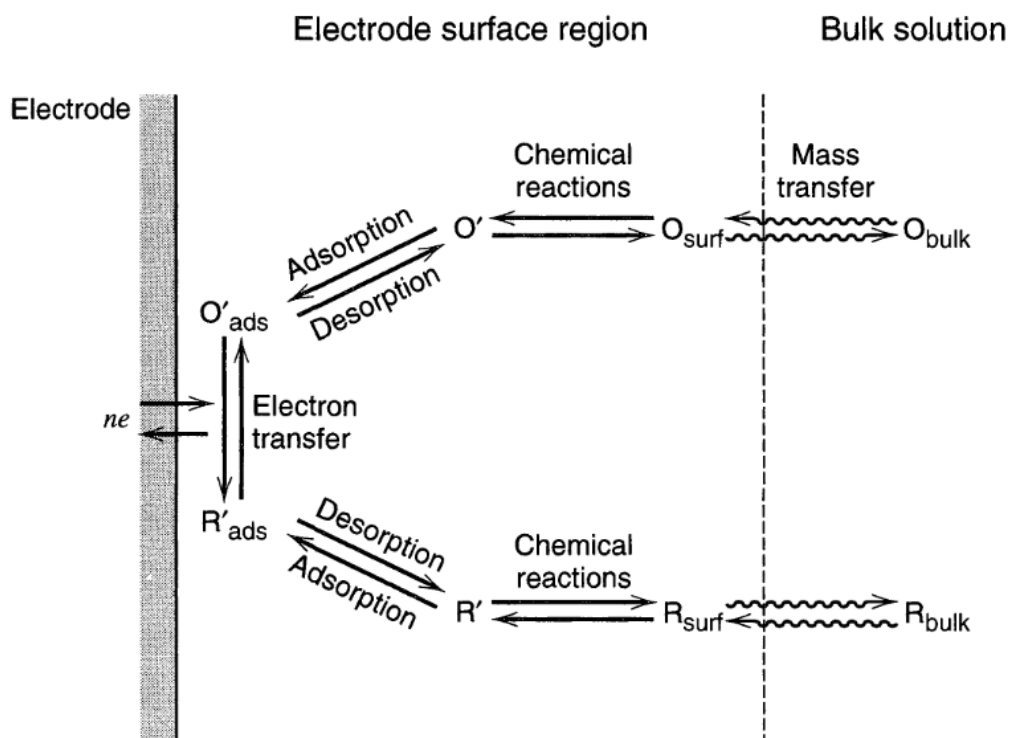


Figure 5: Pathway of a general electrode reaction. Adopted from <sup>50</sup>

### 1.5 Problem statement

Currently, the biomarkers of the body appeared as a powerful tool to improve the prevention, detection and treatment of different deceases and degenerative disorders. Neurotransmitter are one of the most important because they regulate the mayor part of cell and tissue function. Some of them include the Dopamine (DA) which have fundamental role in cardiovascular, kidney, central nervous and hormonal system regulation <sup>36</sup>. Besides, abnormal concentration of DA generated diseases such as cancer, Parkinson, Huntington, dementia <sup>35</sup> and trend to drug dependence <sup>39</sup>. In the case of Serotonin (SER), it has strong influence in the mood and sleep regulation <sup>65</sup>. Schizophrenia, depression, drug addiction and others neuropsychiatric disorders are some of the symptoms of imbalance of SER <sup>23</sup>. Another important neurotransmitter is Epinephrine which is known as alert hormone because it boosts the supply of oxygen and glucose to the brain and muscles in emergency situations. Similar to Dopamine its level in body are related to Parkinson disease <sup>47</sup> but it also has therapeutic application for asthma, sepsis, severe allergic, cardiac arrest and anaphylaxis <sup>66</sup>. On the other hand, uric acid levels in human body provide information about the metabolic alterations or diseases such as Metabolic Syndrome, Hypertension, Kidney Injury, and Cardiovascular <sup>67</sup> because it is the final product

of different metabolic pathways <sup>5</sup>. In that context, electrochemical sensor base on CP appears as cheaper, effective and sensitive alternative for detecting those molecules in human fluids.

In this work, an extensive literature review is reported focusing in the state-of-the-art of the CP based electrochemical sensors for detection of dopamine, epinephrine, serotonin and uric acid. The formation of nanostructures during the synthesis of the CPs is explored resulting in mesoporous and microporous structures with large surface areas that involve fast electron transfer and increased sensitivity <sup>64</sup>.

## **1.6 General and specific objectives**

### **- General objective**

To generate a state-of-the-art review in the conducting polymers based electrochemical sensors for detection of different organic molecules in solution.

### **- Specific objectives**

To compile and analyze the most relevant reported research about electrochemical sensors based on conducting polymer for detection dopamine in solution published since 2015.

To compile and analyze the most relevant reported research about electrochemical sensor base on conducting polymer for detection serotonin in solution published since 2015.

To compile and analyze the most relevant reported research about electrochemical sensor base on conducting polymer for detection epinephrine in solution published since 2015.

To compile and analyze the most relevant reported research about electrochemical sensor base on conducting polymer for detection uric acid in solution published since 2015.

## STATE-OF-THE-ART REVIEW

### 2.1 Dopamine

Selective sensors based on polypyrrole (PPy) have been used for dopamine detection mainly due to environmental stability, good biocompatibility and high surface area <sup>68</sup>. Furthermore, polypyrrole is easily synthesized and shows higher conductivity in comparison with other conducting polymers <sup>69</sup>. The amine group (–NH–) on the pyrrole ring enhances the capability of this polymer for biomolecular sensing <sup>70</sup> and provides a non-sensitive character to interferences in the solution <sup>71</sup>. The PPy base sensor for dopamine were analyzed above:

Poly- pyrrole films doped with anionic sulfonated  $\beta$ -cyclodextrin (PPy-S $\beta$ CD) were potentiostatically deposited on platinum electrodes <sup>72</sup>. The obtained films showed a structure with ridges and valleys which generate ladder-like arrangement. LOD of 1  $\mu$ M were chronoamperometrically determined for dopamine at NaCl solutions. Moreover, this modified electrode showed a high selectivity for dopamine due to a strong interaction between cyclodextrin dopant and the protonated DA.

A hybrid sensor base on graphene oxide and overoxidized electropolymerized polypyrrole (OPPy/ERGO) onto a glassy carbon electrode was made for selective detection of dopamine <sup>73</sup>. First, reduced graphene was prepared by cyclic voltammetry in a graphene oxide / PBS solution at pH 7.4. Then, PPy was potentiodynamically deposited from a pyrrole solution. SEM analysis showed pristine PPy/ERGO deposits had laminated and spherical structures (attributed to PPy). After overoxidation in a NaOH solution, a rough, uniform and compact thin film was obtained with incorporation of carbonyl groups. LOD was determined by amperometric measurements resulting a value of 0.2  $\mu$ M with a linear response between 0.4  $\mu$ M and 517  $\mu$ M. Negatively charged sensor surface allowed for the absorption of positively charged dopamine. A similar approach was taken by Demirkan et al. where palladium nanoparticles supported on polypyrrole/reduced graphene oxide (rGo/Pd@PPy NPs) were developed for ascorbic acid, dopamine, and uric acid sensing <sup>74</sup>. rGo/Pd@PPy NPs nanocomposite. TEM images of rGo/Pd@PPy NPs nanocomposites showed spherical Pd nanoparticles distributed under the polymeric film. Limit of detection (LOD) by DPV for ascorbic acid, dopamine, and uric acid were  $4.9 \times 10^{-8}$  M,  $5.6 \times 10^{-8}$  M,  $4.7 \times 10^{-8}$  M, respectively within a range of  $1 \times 10^{-3}$  M -  $1.5 \times 10^{-2}$  M. This sensor shows electrocatalytic performance, effective electron transfer capability, and better sensitivity because of synergistic effects of its component.

Hybrid composite of molybdenum oxide-based three-dimensional MOFs with helical channels combined with polypyrrole ( $\text{CuTRZMoO}_4\text{@PPy-n}$ ) were tested for dopamine detection by Zhou et al.<sup>68</sup>. Polypyrrole was employed in order to boost the conductivity of the preset metal-organic framework (MOF). Structural analysis reveals a coarse, irregular and circular fringe nanocomposite surface. DPV allowed for an 80 nM detection limit and 1  $\mu\text{M}$  to 100  $\mu\text{M}$  linear range in a PBS pH 2.5 solution.

ZnO nanotubes supported on molecularly imprinted polymers arrays (MIPs/ZNTs/FTO glass) were used for dopamine detection<sup>38</sup>. Zn nanorods (ZNRs) were deposited by potentiostatic methods onto fluorine-doped tin oxide (FTO). Then, ZNRs were tuned into Zn nanotubes (ZNT) by chemical etching in alkaline solution at low temperatures. Polypyrrole films were electrodeposited from a solution of the monomer, lithium perchlorate and dopamine. Finally, the electrode was potentiodynamic cleaned in PBS to oxidase and eliminate the embedded dopamine. SEM images showed cylindrical ZNT coated with PPy films. A high selectivity for dopamine was reported because this molecule was used as template for molecular printing (see Figure 6).

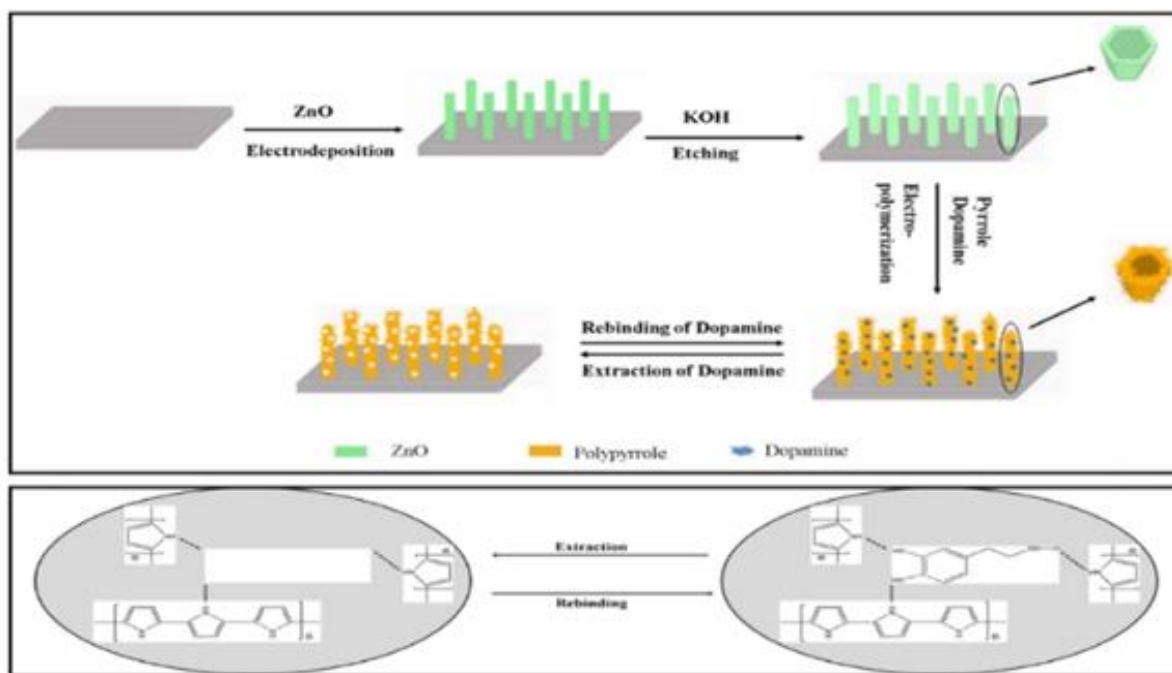


Figure 6: Graphical description of synthesis process of composite MIPs/ZNTs/FTO glass.

Adopted from<sup>38</sup>

PPy/C#SiO<sub>2</sub> nanocomposite was synthesized using a mixture of pyrrole and previous manufactured carbon-coated mesoporous SiO<sub>2</sub> composite (C#SiO<sub>2</sub>)<sup>75</sup>. The deposition of PPy

was confirmed using WAXD and FTIR. LOD of  $7.6 \times 10^{-7}$  M was determined by DPV within a linear range of  $1 \times 10^{-6}$  M -  $2 \times 10^{-4}$  M. This electrode showed a small charge-transfer resistance as a result of synergetic effect of compounds.

Overoxidized polypyrrole / sodium dodecyl sulfate (SDS)-modified multi-walled carbon nanotube (OPPy/SDS-CNT) composites were assembled on gold electrodes by potentiostatic techniques <sup>76</sup> . After polypyrrole co-deposited with SDS and MWCNT, electrodes were overoxidized in a NaOH for generated carboxylic and carbonyl groups in composite surface. Field emission scanning electron microscopy (FESEM) images showed a rough surface in the pristine deposit due to aggregates of PPy/SDS-CNT which partially disappeared by overoxidation. Dopamine in phosphate buffer solution was detected by differential pulse voltammetry (DPV) showing a linear range from 5 nM to 10 nM and a limit of detection (LOD) of 136 pM. The high sensibility of this method is attributed to electrostatic interaction between positively charged dopamine and negatively charged OPpy/SDS-CNT electrode.

Nanocomposite of polypyrrole and silver nanoparticles (PPy-Ag) have been also used for dopamine sensing <sup>77</sup> . Black solid particles of PPY-Ag nanocomposite were synthesized (see Figure 7) and further studied by SEM and TEM. The PPy-Ag showed a rod-like structure with embedded spherical Ag nanoparticles. Detection limit of 50 pM and linear range from 0.00005  $\mu$ M to 0.003  $\mu$ M was obtained for dopamine using linear sweep voltammetry (LSV) in a solution of PBS at pH 7. A better electroactive surface which facilitates the tunneling of electrons within the redox couple is the responsible of this quite high sensitivity. Moreover, biocompatibility essay was performed in mouse fibroblast cell exhibiting low toxicity.

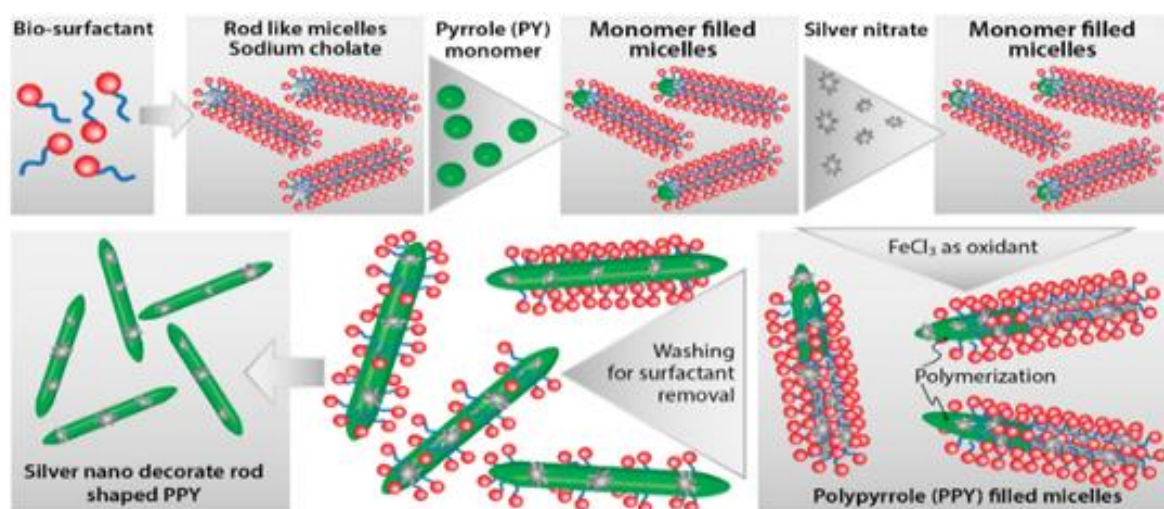


Figure 7: Graphical description of synthesis process of composite PPY-Ag. Adopted from <sup>77</sup>

On the other hand, polyaniline (PANI) appears as one of the most used CP materials for sensors assemble. PANI present interesting properties such as stability, flexibility, good electrical and optical properties<sup>78</sup> and have functional groups in the surfaces that improves the absorption of analytes<sup>79</sup>. A low cost and high yield manufacturing process<sup>80</sup> and possibility to switch between the insulating and conducting phases by acid/base process<sup>81</sup> make this PANI one of the most versatile material for application in the sensing field.

Polyaniline films has been also used in the detection of dopamine. Polyaniline-Au (PANI-Au) nanocomposite dopamine sensors were fabricated by combined acid and oxidative doping pathways<sup>82</sup>. These composites were synthesized using different pathways in liquid phase which are shown in Figure 8. Ammonium persulphate (APS) and chloroauric acid (HAuCl<sub>4</sub>) were employed as oxidant agents while p-toluene sulphonic acids (pTSA) and sulfuric acid were used as protonic acid dopants. SEM images showed PANI-H<sub>2</sub>SO<sub>4</sub> had dense nature while PANI-pTSA had layered morphology with high porosity. Spherical Au nanostructures were deposited over polymeric films PANI-H<sub>2</sub>SO<sub>4</sub>@Au sensors gave a LOD of 6.7 μM within a linear range of 10 μM - 100 μM while PANI- pTSA@Au sensors gave a LOD of 5.25 μM within a linear range of 7 μM - 100 μM. These sensors generated well-defined signals allowing for a selective sensing of dopamine in presence of interferences.

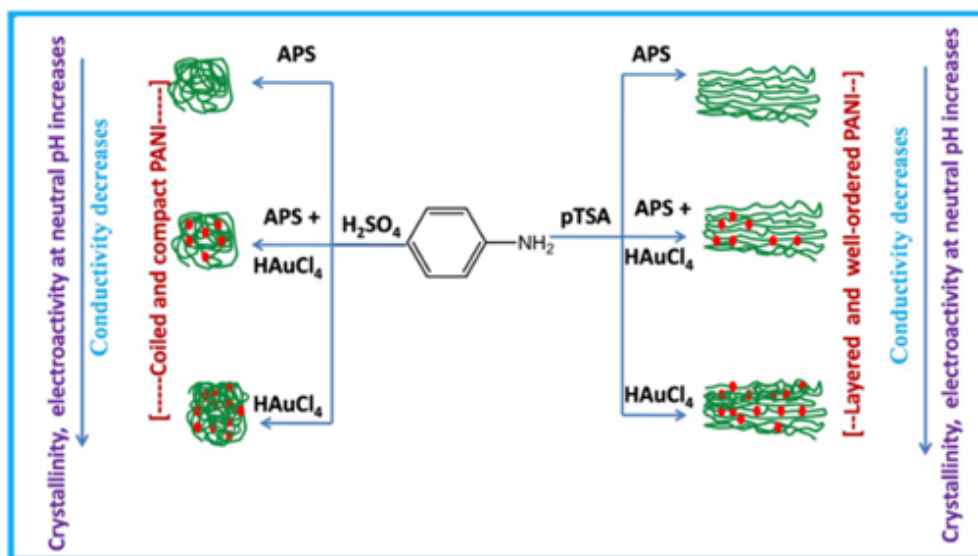
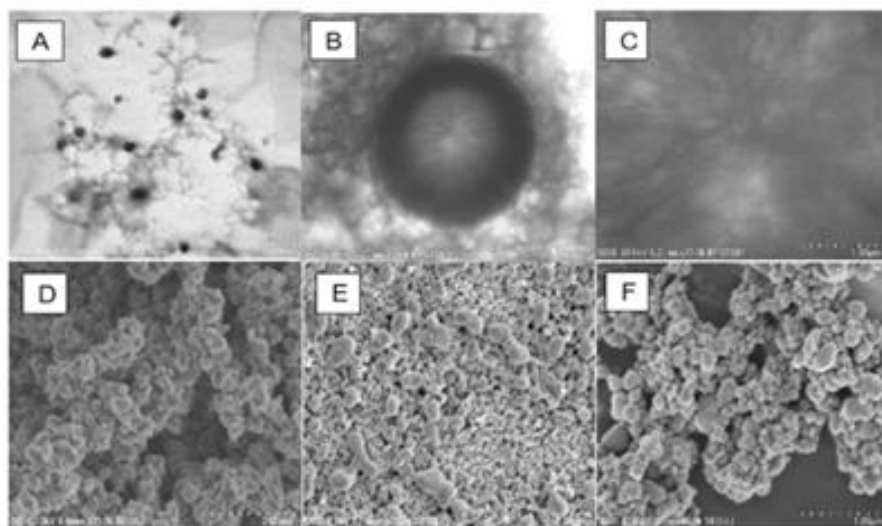


Figure 8. Grafical representation of different synthesis pathways for manufacturing the composite PANI-pTSA. Adopted from<sup>82</sup>

Polyaniline deposited over glassy carbon has been also used as support in the electropolymerization of beta-cyclodextrin (β-CD) / hydroxyl functionalized multi-walled

carbon nanotubes (f-MWCNTs) in PBS solution at pH 7<sup>83</sup>. Morphology was analyzed by FESEM and TEM techniques as is showed in Figure 9. Poly- $\beta$ -CD(f-MWCNTs)/PANI nanocomposite showed a porous granular morphology taken after PANI support resulting in high surface area. Poly- $\beta$ -CD showed a globular structure. LOD of 0.0164  $\mu$ M was determined by DPV. The sensitivity obtained for this electrode was ascribed to the high porosity and high surface area.



*Figure 9: TEM images of different films of composite Poly- $\beta$ -CD(f-MWCNTs)/PANI where is possible to observe the different morphologies of its layers . Adopted from<sup>83</sup>*

A sensor based on a derivative of poly (o-methoxyaniline)-gold (POMA-Au) nanocomposites. showed a LOD of 0.062  $\mu$ M within a linear range from 10  $\mu$ M to 300  $\mu$ M for dopamine<sup>84</sup>. POMA provided a large surface area and Au nanoparticles high electrical conductivity.

Poly(aniline-co-o-anisidine)/graphene oxide nanocomposites coated with Au nanoparticles (AuNPs/PANI-co-PoAN/GO) was also fabricated for dopamine sensing applications<sup>85</sup>. A copolymer of aniline and o-anisidine was synthesized by adding ammonium persulfate to a solution of hydrochloric acid containing both monomers and graphene oxide. Au electrodes were dipped coated in PANI-co-PoAN/GO diluted in chloroform followed by potentiodynamic deposition of Au nanoparticles KCl / HAuCl<sub>4</sub> solution. LOD for dopamine using SWV was 0.0334  $\mu$ M within a linear range of 5  $\mu$ M - 100  $\mu$ M. This sensor showed a fast electron transfer and high surface area due to Au nanoparticles.

Poly(N-( Naphthyl) ethylenediamine dihydrochloride) nanofibers on anodized glassy carbon electrodes (PNEDA/AGCE) were developed as dopamine electrochemical sensor by Rahman

et al. <sup>86</sup>. DPV with dopamine concentrations in the range of 0.1  $\mu\text{M}$  - 100  $\mu\text{M}$  gave a LOD of 0.070  $\mu\text{M}$ . DFT calculations showed a strong H-bonding interaction between the free  $-\text{NH}_2$  groups of PNEDA and oxidizable  $-\text{OH}$  groups of DA resulting in the high sensitivity for this sensor.

Graphene/poly(o-phenylenediamine) (GP/PoPD) was potentiodynamically deposited onto pencil graphite electrodes (PGE) from lithium perchlorate, o-phenylenediamine and graphene solution <sup>87</sup>. LOD of 0.16 nM was obtained by SWV within a linear range of  $1.0 \times 10^{-3}$   $\mu\text{M}$  - 150  $\mu\text{M}$ . This low LOD was ascribed to a high electroactive surface area and fast electron transfer.

A highly selective sensor for dopamine was developed using poly-4-Amino-6-hydroxy-2-mercaptopyrimidine (Poly-AHMP) film over glassy carbon electrode <sup>88</sup>. A highly rough and porous surface was observed in SEM images of film resulting in an increased active surface area of electrode. This sensor showed a LOD of 0.2  $\mu\text{M}$  within a linear range from 2.5  $\mu\text{M}$  to 25  $\mu\text{M}$  by DVP.

Different polythiophene derivatives has shown potential in the fabrication of dopamine sensors <sup>89 90</sup> among them poly(3,4-ethylenedioxythiophene (PEDOT) is considered a top-choice due to high electrical conductivity which is just on order of magnitude of silver and copper <sup>91</sup>, huge optical transparency at visible light and better room stability than PPy<sup>92</sup>. Furthermore, PEDOT present extraordinary redox reversibility<sup>93</sup> which provide antifouling properties that expands the using time life of polymer film <sup>92</sup>. Additionally, PEDOT has the advantage of easy synthesis process<sup>94</sup> and generate deposition with low tensile module allowing support constant mechanical deformation generally relate to biological application <sup>95</sup>.

PEDOT-Modified Laser Scribed Graphene (PEDOT-LSG) electrodes were used as electrochemical sensor for dopamine <sup>96</sup>. LSG had regular and smooth flake structure which after PEDOT electropolymerization a 3D porous network structure remains (see Figure 10). A detection limit of 0.33  $\mu\text{M}$  within a linear range of 1  $\mu\text{M}$  - 150  $\mu\text{M}$  was obtained by DPV in PBS solution at pH 7. Sensitivity of this sensor was related to the rapid electron transport properties of porous graphene combined with the electrocatalytic activity of PEDOT deposit.

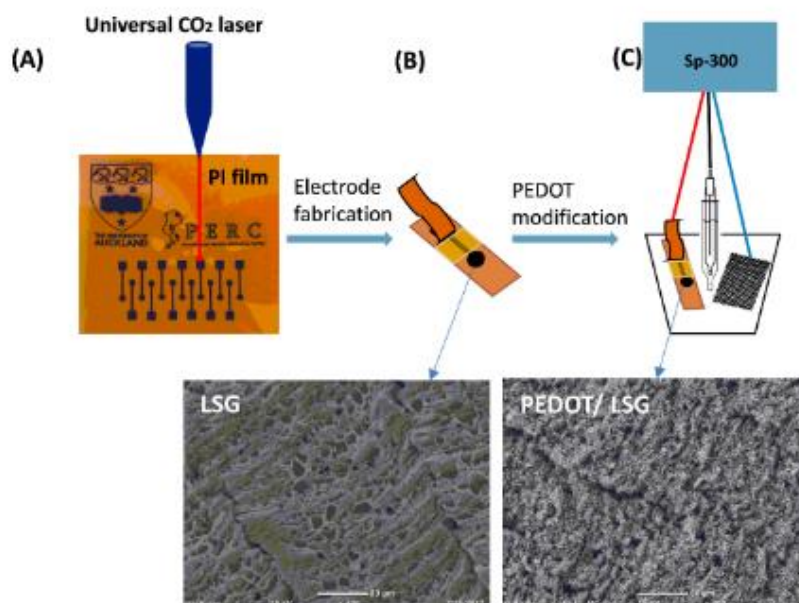


Figure 10: Graphical description of synthesis of composite PEDOT-LSG and its morphology studies that shows the porosity of film. Adopted from <sup>96</sup>

Sandoval-Rojas et al. fabricated poly(3,4-ethylenedioxythiophene) doped with a bis(pyrazolyl)methane disulfonate sensors (PEDOT/LSA) for detection of dopamine <sup>97</sup>. This electrode was synthesized over glassy carbon electrode using potentiodynamic voltammetry in an EDOT and sodium salt of bis(3,5-dimethyl-4-sulfonate-pyrazol-1-yl)methane in acetonitrile / deionized water mixtures. The dopant produced large globular structures on the polymer surface. A LOD of 0.26  $\mu\text{M}$  within a linear range from 0  $\mu\text{M}$  to 5  $\mu\text{M}$  was obtained using DPV.

Monodispersed poly(3,4-ethylenedioxythiophene) / gold hollow nanospheres (PEDOT/Au) electrodes were designed for DA sensing <sup>98</sup>. The composite was synthesized over glassy carbon electrode in aqueous phase. Hollowed nanospheres template was precipitated from a stirred  $\text{Na}_2\text{S}_2\text{O}_3$  / PVP solution. Then PEDOT / Au hollow nanospheres were produced by stirring PVP modified sulfur nanospheres in an EDOT /  $\text{HAuCl}_4$  solution as Figure 11 shows. SEM micrographs revealed a 3D globular structure with size of 300 nm to 1000 nm. Linear range and LOD values of 0.15  $\mu\text{M}$  to 330  $\mu\text{M}$  and 0.07  $\mu\text{M}$ , respectively, were reported by using DPV. Excellent performance of this electrode is ascribed to fast electron charge transfer kinetics of this composite.

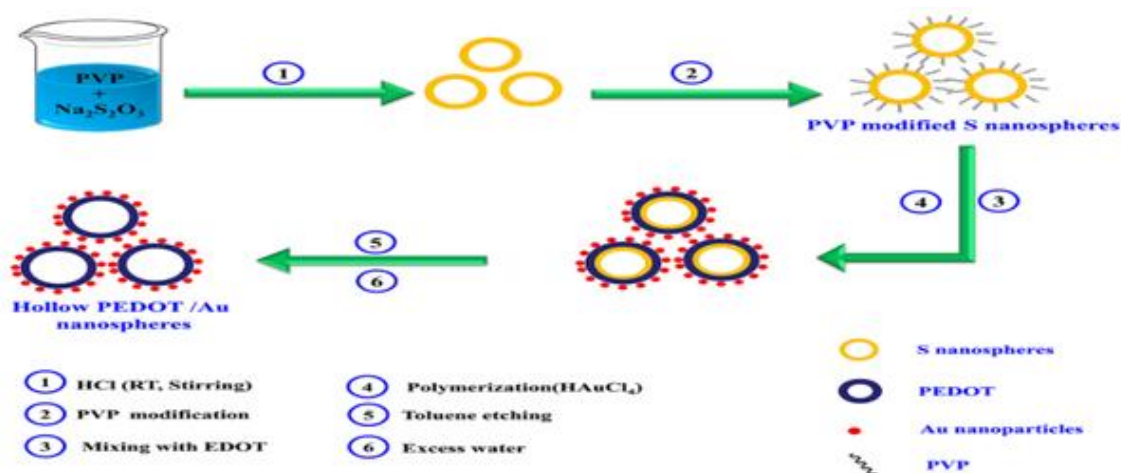


Figure 11: Graphical synthesis process of PEDOT/Au. Adopted from <sup>98</sup>

Composites of multi-walled carbon nanotubes and nanoceria-poly(3,4-ethylenedioxythiophene) (MWCNTs/CeO<sub>2</sub>-PEDOT) were also used for dopamine detection <sup>99</sup>. PEDOT films agglomerated into sphere-like grains preserving this structure in the composite with particles diameters between 200 nm and 450 nm. A detection limit of 0.03  $\mu\text{M}$  within a linear range of 0.1  $\mu\text{M}$  - 10  $\mu\text{M}$  was determined by DPV measurements.

Poly(3,4-ethylenedioxythiophene) / reduced graphene oxide / manganese dioxide modified glassy carbon electrodes (PrGO/MnO<sub>2</sub>) were built for simultaneous detection of DA, Uric acid (UA) and ascorbic acid (AA) <sup>100</sup>. After potentiodynamic electrodeposition of PrGO on glassy carbon electrode, MnO<sub>2</sub> was deposited using a solution of KMnO<sub>4</sub> and H<sub>2</sub>SO<sub>4</sub>. PEDOT appears as granular film deposited over rGo. The MnO<sub>2</sub> is observed as small particles onto PrGO. Sensor structure provided a high surface area which increases the sensitivity. This composite shows high electrocatalytic activity that generated a well-separated oxidation potential of UA, DA and AA. Simultaneous detection gave LOD values of 0.05  $\mu\text{M}$  (UA), 0.02  $\mu\text{M}$  (DA) and 1  $\mu\text{M}$  (AA) in PBS at pH 6.

Poly(3,4-ethylenedioxythiophene) doped with ionic liquid (1-ethyl-3-methylimidazolium bis(trifluoromethylsulfonyl)imide) on glassy carbon electrode (PEDOT/IL/GCE) have been also used as biofouling resistant dopamine electrode showing porous microstructure, high electrical conductivity and good stability <sup>101</sup>. LOD and linear range values of 33 nM and 0.2  $\mu\text{M}$  to 328  $\mu\text{M}$ , respectively, were found for dopamine sensing in presence of proteins such as BSA, HSA and LZM.

Spin coated poly(3, 4-ethylenedioxythiophene):polystyrene functionalized with beta-cyclodextrin sensors (CD-f-PEDOT:PSS) for dopamine and catechol were fabricated by Qian

et al.<sup>102</sup>. AFM images showed PEDOT: PSS surface changes by treatment with H<sub>2</sub>SO<sub>4</sub> from polymer particles to entangled wires boosting the electrical conduction. The obtained detection limit and linear range were 0.009596 μM and 0.05 μM to 200 μM, respectively, by using DPV in a PBS buffer at pH 7.4

Highly sensitive dopamine sensor were developed by Pananon et al. using a nanocomposite made of gold nanoparticles, graphene (GP) and poly (3,4-ethylenedioxythiophene):polystyrene sulfonate ( AuNP-GP-PEDOT:PSS/GCE) using a green synthetic method<sup>103</sup>. SEM images proved an uniform distribution of gold nanoparticles in the surface. This sensor shows a quite low detection limit (100 pM within linear dynamic ranges from 1 nM to 300 μM) because an increased surface area, high catalytic activity of AuNP and a superior conductivity of GP and PEDOT:PSS.

Moreover, thin polythiophene films composed with gold nanoparticles and carbon nanotubes (PT/Au/CNT) were synthesized by liquid-liquid interfacial reaction<sup>104</sup>. The construction of this composite required an aqueous mixture of dispersed CNT, HCl, HAuCl<sub>4</sub>.3H<sub>2</sub>O and thiophene (in a molar relation 1:1 with HAuCl<sub>4</sub>). Modified electrodes were self-assembled by putting a substrate (silicon, quartz or glass) in a stirred solution for 4.5 hours as shown in Figure 12. This method resulted in a detection limit of 0.69 μM for DA by DPV. These results point out for an enhanced charge transfer related to the presence of CNT.

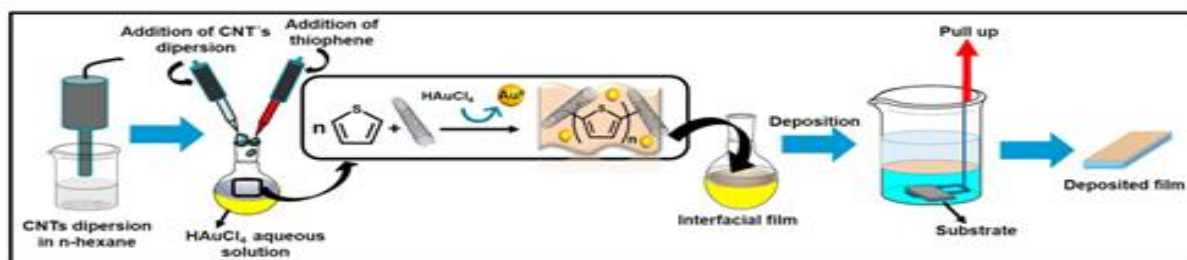


Figure 12: synthetic process of composite PT/Au/CNT. Adopted from<sup>104</sup>

Unconventional conducting polymers have been also used for DA sensing. Poly (sudan III) was potentiodynamically deposited over carbon paste electrodes (PS/MCPE) in a solution containing NaOH and Sudan III<sup>105</sup>. SEM images showed irregularly shaped graphite flakes at the surface. A detection limit of 9.3 μM (linear range of 10 μM - 90 μM) was determined by DPV.

Poly phenol red film on glassy carbon electrode was used for detection of dopamine and acetaminophen<sup>106</sup>. Potentiodynamic polymerization of this molecule is possible through

quinone methide group. Sensing experiments were carried out in PBS at different pH. Detection limit and linear range for dopamine (DA) were 1.6  $\mu\text{M}$  and 20  $\mu\text{M}$  - 160  $\mu\text{M}$ , respectively. The value of catalytic rate constant ( $8.45 \times 10^2 \text{ M}^{-1} \text{ S}^{-1}$ ) demonstrates that p-PhR/GCE has a catalytic oxidative reaction for dopamine.

Poly (procateterol hydrochloride) modified glassy carbon electrodes (p-ProH/GCE) were used for dopamine and uric acid detection in human serum <sup>107</sup>. These sensors were built by potentiodynamic method in a PrOH solution on glassy carbon electrodes. Modified electrodes showed a high affinity for dopamine with a detection limit value of 0.3  $\mu\text{M}$  within a linear range of 1  $\mu\text{M}$  - 100  $\mu\text{M}$  by square wave voltammetry (SWV) in PBS at pH 5.

Composites of poly(glyoxal-bis(2-hydro- xyanil) , amino-functionalized graphene quantum dots and  $\text{MnO}_2$  nanoclusters were deposited over glassy carbon electrodes (GCE/PGBHA-afGQDs- $\text{MnO}_2$ ) for vitamin B12 and dopamine sensing <sup>108</sup>. SEM images displayed rough and dense film with GQDs clusters made of particles particles with zise less than 50 nm which increase the roughness hence the surface area and electroconductivity resulting in LOD of 0.05  $\mu\text{M}$  for DA by DPV.

Poly (hydroquinone)/gold nanoparticles/nickel foam (pHQ/AuNPs/NF) were used for dopamine sensitive detection<sup>109</sup>. First, gold nanoparticles were deposited over previously cleaned nickel foam by potentiostatic methods in a solution containing  $\text{HAuCl}_4$ . Then potentiodynamic polymerization of hydroquinone was performed in phosphate buffered solution at pH 5 (see Figure 13). Micrographs showed the porous 3D network structure of NF with a rough surface due to the deposited pHQ / AuNPs. These modifications of Nickel foam provide a large surface area and high conductivity. Determination of dopamine was made using DPV resulting in a detection limit and linear range of  $4.19 \times 10^{-8} \text{ M}$  and  $1.0 \times 10^{-7} \text{ M}$  to  $1.0 \times 10^{-5} \text{ M}$  respectively.

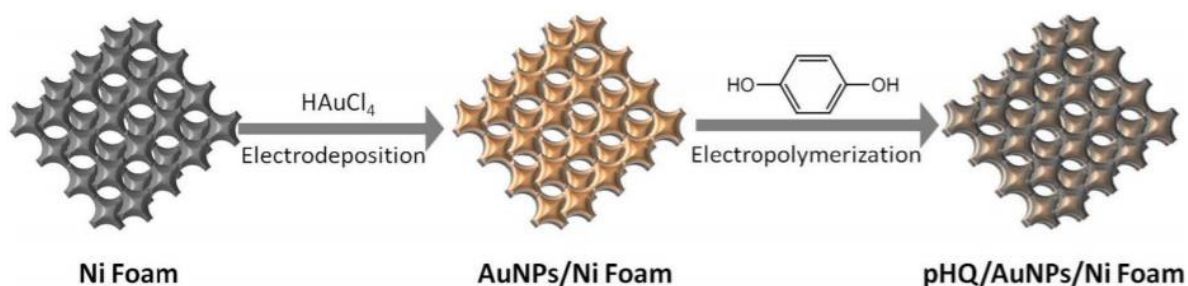


Figure 13: Graphical process of deposition of pHQ/AuNPs over Ni Foam. Adopted from 109

Ascorbic acid, dopamine and uric acid detection was performed using a sensor base on electrochemical reduced graphene oxide-poly (eriochrome black T) / gold nanoparticles (ERGO-pEBT/AuNPs) modified glassy carbon electrodes <sup>110</sup>. FESEM technique showed a uniformly rough composite surface with Au nanoparticles homogeneously distributed leading to LOD values of 0.009  $\mu\text{M}$  (within a linear range of 0.5  $\mu\text{M}$  - 20  $\mu\text{M}$ ) for DA.

Carboxylic acid functionalized multi-walled carbon nanotubes / polytoluidine blue over glassy carbon electrodes (MWCNTs-COOH/Poly(TB)/GCE) showed high sensitivity to DA (LOD = 0.39 nM) related to the high surface area of the net-structure MWCNTs-COOH and the electrocatalytic activity of polymer <sup>111</sup>.

Arroquia et al. fabricated self-assembled gold-decorated-polydopamine nanospheres (Au PDNs) for simultaneous detection of ascorbic acid, dopamine, uric acid and tryptophan <sup>112</sup>. First, synthesis of polydopamine nanospheres (PDNs) involved a 3 hour stirring in dopamine hydrochloride / NaOH solution at 50°C. Suspension of PDNs was mixed with HAuCl<sub>4</sub> and ascorbic acid to get Au nanospheres (Au-PDNs) Finally, Au-PDN composite was covered onto screen-printed carbon electrode previously modified with gold nanoparticles, cysteamine and glutaraldehyde (see Figure 14). Electronic microscopy showed a homogeneous distribution of Au-PDN nanospheres onto modified electrode resulting in high surface areas with an improved charge transfer process. A low LOD of 0.1 nM was determined for DA with a linear range from 1  $\mu\text{M}$  to 160  $\mu\text{M}$  by DPV.

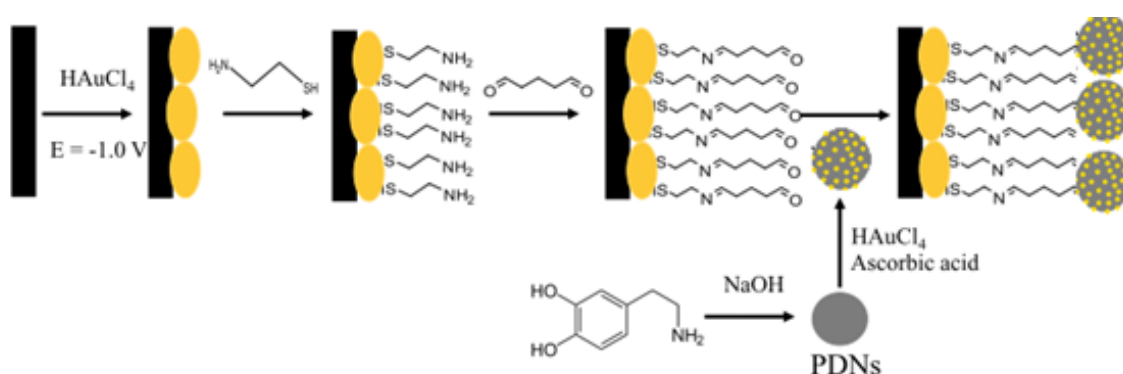


Figure 14: Graphical representation about the assemble of different layer of Au-PDNs electrode. Adopted from <sup>112</sup>

Table 1: Comparison of figures of merit conducting polymer-based sensors for the detection DA

Electrode Materials	Polymer	Synthesis Method	Analytes	Detecting technique	LOD ( $\mu\text{M}$ )	Linear range ( $\mu\text{M}$ )	Ref.
pHQ/AuNPs/NF	Poly (hydroquinone)	CV	DA	DPV	0.0419	0.1 to 10	<sup>109</sup>
p-ProH/GCE)	Poly (procaterol hydrochloride)	CV	DA, UA	SWV	0.3	1 to 100	<sup>107</sup>
PS/MCPE	Poly (sudan III)	CV	DA	DPV	9.3	10 to 90	<sup>105</sup>
MWCNTs-COOH/Poly(TB)/GCE)	Poly (toluidine blue)	CV	DA	DPV	0.00039	1 to 300	<sup>111</sup>
Poly phenol red/GCE	Poly phenol red	CV	DA, Acetaminophen	DPV	1.6	20 to 160	<sup>113</sup>
CD-f-PEDOT: PSS	Poly (3,4-ethylenedioxythiophene) polystyrene sulfonate	Spin coating technique	DA, catechol	DPV	0.009596	0.05 to 200	<sup>102</sup>
AuNP-GP-PEDOT:PSS/GCE	Poly (3,4-ethylenedioxythiophene) polystyrene sulfonate	Self-assembled / liquid phase	DA	DPV	0.0001	0.001 to 300	<sup>103</sup>
ERGO-pEBT/AuNPs	Poly (eriochrome black T)	CV	DA, UA, AA	DPV	0.009	0.5 to 20	<sup>110</sup>

<b>Electrode Materials</b>	<b>Polymer</b>	<b>Synthesis Method</b>	<b>Analytes</b>	<b>Detecting technique</b>	<b>LOD (<math>\mu\text{M}</math>)</b>	<b>Linear range (<math>\mu\text{M}</math>)</b>	<b>Ref.</b>
POMA-Au	Poly (o-methoxyaniline)	Self-assembled/liquid phase	DA, Folic acid	DPV	0.062	10 to 300	84
PrGO/MnO <sub>2</sub>	Poly(3,4-ethylenedioxythiophene)	CV	DA, UA, AA	DPV	0.02	0.03 to 45	100
PEDOT/Au	Poly(3,4-ethylenedioxythiophene)	Self-assembled/liquid phase	DA, UA	DPV	0.07	0.15 to 330	98
PEDOT/LSA	Poly(3,4-ethylenedioxythiophene)	CV	DA	DPV	0.26	0 to 5	97
MWCNTs/CeO <sub>2</sub> -PEDOT	Poly(3,4-ethylenedioxythiophene)	Self-assembled/liquid phase	DA	DPV	0.03	0.1 to 10	99
PEDOT/IL/GCE	Poly(3,4-ethylenedioxythiophene)	CV	DA	CV	0.33	0.2 to 328	101
PEDOT-LSG	Poly(3,4-ethylenedioxythiophene)	Chronoamperometry	DA	DPV	0.33	1 to 150	96

<b>Electrode Materials</b>	<b>Polymer</b>	<b>Synthesis Method</b>	<b>Analytes</b>	<b>Detecting technique</b>	<b>LOD (<math>\mu\text{M}</math>)</b>	<b>Linear range (<math>\mu\text{M}</math>)</b>	<b>Ref.</b>
AuNPs/PANI-co-PoAN/GO	Poly(aniline-co-o-anisidine)	Self-assembled/liquid phase	DA	SWV	0.0334	5 to 100	85
GCE/PGBHA-afGQDs-MnO <sub>2</sub>	Poly(glyoxal-bis(2-hydroxy-xyanil))	CV	DA	DPV	0.05	0.1 to 100	108
PNEDA/AGCE	Poly(N-(Naphthyl)ethylenediamine dihydrochloride)	Chronoamperometry	DA	DPV	0.070	0.1 to 100	86
GN/PoP	Poly(o-phenylenediamine)	CV	DA	SWV	0.00016	0.001 to 150	87
Poly-AHMP	Poly-4-Amino-6-hydroxy-2-mercaptopyrimidine	CV	DA, Acetaminphen	DPV	0.2480	2.5 to 25	88
Poly- $\beta$ -CD(f-MWCNTs)/PANI	Polyaniline	CV	DA	DPV	0.0164	2 to 24	83
PANI-Au	Polyaniline	Self-assembled/liquid phase	DA	DPV	5.25	7 to 100	82

<b>Electrode Materials</b>	<b>Polymer</b>	<b>Synthesis Method</b>	<b>Analytes</b>	<b>Detecting technique</b>	<b>LOD (<math>\mu\text{M}</math>)</b>	<b>Linear range (<math>\mu\text{M}</math>)</b>	<b>Ref.</b>
Au-PDNs	Polydopamine	Self-assembled/liquid phase	DA, UA, AA, tryptophan	DPV	0.0001	1 to 160	<sup>112</sup>
OPPy/SDS-CNT	Polypyrrole	Chronoamperometry	DA	DPV	0,000136	0,005 to 0,010	<sup>76</sup>
PPy-S $\beta$ CD	Polypyrrole	Chronoamperometry	DA	Chronoamperometry	1	N/A	<sup>72</sup>
CuTRZMoO <sub>4</sub> @PPy-n	Polypyrrole	Self-assembled/liquid phase	DA	DPV	0.08	1 to 100	<sup>68</sup>
MIPs/ZNTs/FTO glass	Polypyrrole	CV	DA	DPV	N/A	0.02 to 5	<sup>38</sup>
(PPY)-Ag	Polypyrrole	Self-assembled/liquid phase	DA	LSV	0.00005	0.00005 to 0.003	<sup>77</sup>
rGo/Pd@PPy NP	Polypyrrole	Self-assembled/liquid phase	DA, UA, AA	DPV	0.056	1000 to 15000	<sup>74</sup>
OPPy/ERGO	Polypyrrole	CV	DA	DPV	0.2	0.4 to 517	<sup>73</sup>

<b>Electrode Materials</b>	<b>Polymer</b>	<b>Synthesis Method</b>	<b>Analytes</b>	<b>Detecting technique</b>	<b>LOD (<math>\mu\text{M}</math>)</b>	<b>Linear range (<math>\mu\text{M}</math>)</b>	<b>Ref.</b>
PPy/C#SiO <sub>2</sub>	Polypyrrole	Self-assembled/liquid phase	DA	DPV	0.76	1 to 100	<sup>75</sup>
PT/Au/CNT	Polythiophene	Self-assembled/liquid phase	DA	DPV	0.69	1 to 10	<sup>104</sup>

## 2.2 Ephinefrine

Electron beam irradiated polypyrrole nanospheres / bovine serum albumin onto glassy carbon electrodes (EB-PPy-BSA/GCE) were used for epinephrine (EP) and L-tyrosine detection <sup>114</sup>. A mixture of methyl orange, FeCl<sub>3</sub> and pyrrole was used to prepare polypyrrole nanospheres which were treated with electron beam radiation. Polypyrrole nanospheres and bovine serum albumin solution were sonicated for 2 hours followed by dropcasting onto a glassy carbon electrode. SEM and TEM revealed that polypyrrole nanospheres were embedded into porous structure of BSA (see Figure 15). SWV was used for building a calibration curve which gave LOD of  $7.1 \times 10^{-9}$  M and a linear range from  $100 \times 10^{-9}$  M to  $400 \times 10^{-6}$  M. The use of BSA provided large surface area, excellent structure stability, rich pore channels and redox mediator role. Tea, and chicken extract were evaluated with this sensor giving promising results for biological and healthcare applications.

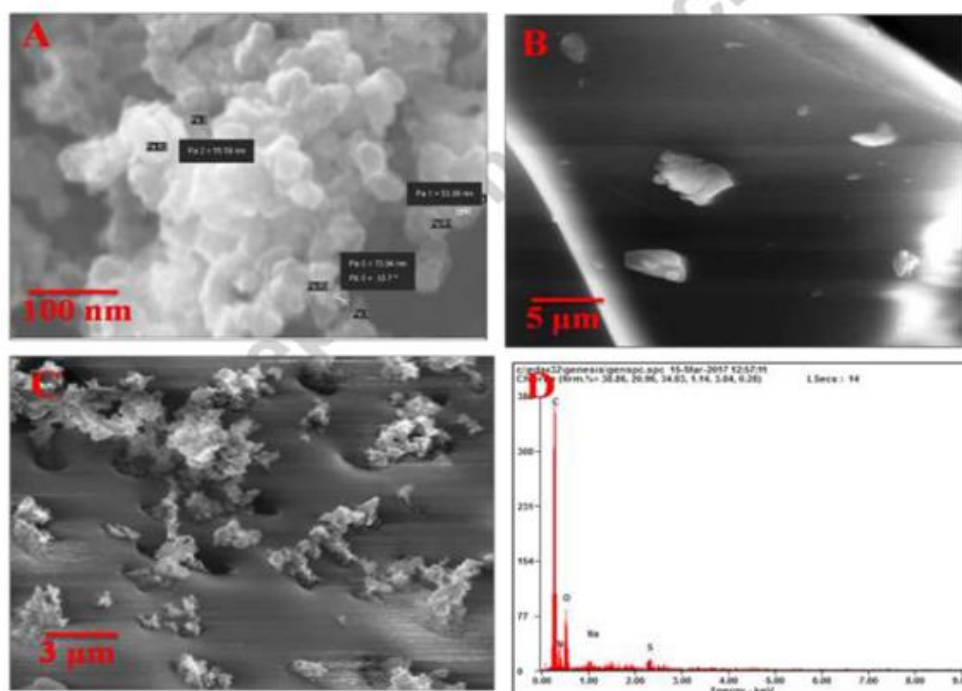


Figure 15: Morphology of different layer of EB-PPy-BSA. a) EB-PPy, b) BSA , c) EB-PPy-BSA and e) EDS spectrum of hybrid structure. Adopted from <sup>114</sup>

Ghanbari and Hajian reported the fabrication of a gold nanoparticles / Zinc oxide / polypyrrole/ reduced graphene oxide nanocomposite (Au /ZnO/PPy/RGO) on glassy carbon electrode for detection of ascorbic acid (AA), epinephrine (EP) and uric acid (UA) <sup>115</sup>. Polypyrrole deposits appeared as nanofibers onto RGO surface. LOD of 0.058 μM and linear range from 0.6 μM to

500  $\mu\text{M}$  was obtained by DPV in PBS solution at  $\text{pH} = 7$ . This sensor was tested in human serum sample giving values mayor of 97 % of recovery.

Three-dimensional mesoporous polymeric graphitic- $\text{C}_3\text{N}_4$ /polyaniline/CdO nanocomposite (mpg- $\text{C}_3\text{N}_4$ /PANI/CdO) was electrochemically synthesized by Bonyadi et al. for simultaneous sensing of epinephrine, paracetamol, mefenamic acid, and ciprofloxacin <sup>116</sup>. FESEM exposed a nanofiber-like that polyaniline structure deposited over the 3D structure made by  $\text{C}_3\text{N}_4$  resulting in tremendous increasing of the electrode surface area. Detection limit of 0.011  $\mu\text{M}$  and two linear ranges from 0.05  $\mu\text{M}$  to 80  $\mu\text{M}$  and from 100  $\mu\text{M}$  to 1000  $\mu\text{M}$  were obtained for epinephrine using DPV in PBS solution at  $\text{pH} = 7.4$ . A 98.9%-102.6% recovery for epinephrine was obtained in human blood serum samples. Polyaniline nanocomposite films has also been doped with  $\text{TiO}_2$  and  $\text{RuO}_2$  nanoparticles on multi-walled carbon nanotubes (MWCNT-PANI- $\text{TiO}_2$  and MWCNT-PANI- $\text{RuO}_2$ ) for epinephrine sensing <sup>117</sup>.  $\text{TiO}_2$  or  $\text{RuO}_2$  nanoparticles, MWCNT and PANI were dissolved in DMF followed by sonication for 24 hours to generate the nanocomposite. This suspension was drop coated onto Au bare electrode. PANI/MWCNT fibers formed tube-like structures with  $\text{TiO}_2$  and spherical shaped particles with  $\text{RuO}_2$  which increases the porosity of composite and its surface area. Calibration curve was performed using DPV in a PBS solution at  $\text{pH} = 7$  with epinephrine concentration from 4.9  $\mu\text{M}$  to 76.9  $\mu\text{M}$ . LODs were 0.16  $\mu\text{M}$  for MWCNT-PANI- $\text{TiO}_2$  and 0.18  $\mu\text{M}$  for MWCNT-PANI- $\text{RuO}_2$ . Both sensors were tested in an epinephrine injection given more than 99% recovery. PANI derivatives such as molecular imprinted poly (3-aminophenylboronic acid) has also been composited with multi-walled carbon nanotubes (PAPBA(MIPs)/MWCNTs) onto glassy carbon electrode for epinephrine sensing showing LODs of 0.035  $\mu\text{M}$  within a linear range of 0.2  $\mu\text{M}$ -800  $\mu\text{M}$ . Molecular printing provides selectivity to distinguish EP from potential interferences <sup>118</sup>. Following a similar strategy, molecularly imprinted poly 3-Thiophene boronic acid (P3-TBA) / gold nanoparticles (MIP/AuNP) composite were developed by Liu and Kan for a selective detection of epinephrine from its analogs <sup>119</sup> resulting in a LOD of  $7.6 \times 10^{-8}$  M by DPV in PBS solution at  $\text{pH} = 7$ . The concentration of EP employed was in the range from  $9.0 \times 10^{-8}$  M to  $1.0 \times 10^{-4}$  M. This sensor had double recognizing ability due to (i) reversible covalent interaction between boronic acid of 3-TBA and cis-diol of EP, and (ii) size and shape complementarity between template molecules and imprinted sites. A 90.6% to 103.5% recovery was obtained in a real epinephrine injection using this sensor.

Au-nanoparticles in poly-fuchsine acid film modified glassy carbon electrodes (poly (FA)/AuNP/GCE) were used for simultaneous detection of ascorbic acid (AA), epinephrine

(EP) and uric acid (UA) <sup>120</sup>. The poly (FA) was deposited by CV from a solution of fuchsine acid and NaOH. Then, AuNPs were electrodeposited by immersing the electrode into a solution of H<sub>2</sub>AuCl<sub>4</sub> and KNO<sub>3</sub>. This electrode had a LOD of 0.01 μM for EP and 0.009 μM for AA in a buffer solution at pH = 3. Moreover, this method was proved in real samples using standard addition method obtained values of 87.0% (in hydrochloride injection) and 102.0% (in urine) of recovery for EP. Potentiodynamic generation of poly (brilliant cresyl blue) on graphene / glassy carbon electrode (PBCB/graphene/GCE) were employed for detection of epinephrine resulting in a detection limit of 0.24 μM by CV in PBS solution at pH = 7 (EP concentration from 1 μM to 1000 μM) <sup>121</sup>.

Table 2: Comparison of figures of merit conducting polymer-based sensors for the detection EP

Electrode Materials	Polymer	Synthesis Method	Analytes	Detection technique	LOD ( $\mu\text{M}$ )	Linear range ( $\mu\text{M}$ )	Ref.
(FA)/AuNP/GCE	poly-fuchsine acid	CV	EP, ascorbic acid, and UA	DPV	0.01	0.5 to 792.7	120
PAPBA(MIPs)/MWCNTs	poly (3-aminophenylboronic acid	CV	EP	DPV	0.035	0.2 to 800	118
MIP/AuNP	3-Thiophene boronic acid	CV	EP,tyrosine	DPV	0.076	0.09 to 100	119
PBCB/graphene/GCE	Poly (brilliant cresyl blue)	CV	EP	Cv	0.24	1 to 1000	121

<b>Electrode Materials</b>	<b>Polymer</b>	<b>Synthesis Method</b>	<b>Analytes</b>	<b>Detection technique</b>	<b>LOD (<math>\mu\text{M}</math>)</b>	<b>Linear range (<math>\mu\text{M}</math>)</b>	<b>Ref.</b>
mpg-C3N4/ PANI/CdO	polyaniline	Chronoamperometry	EP, paracetamol, mefenamic acid, and ciprofloxacin	DPV	0.011	0.05to 80	116
MWCNT-PANI-TiO <sub>2</sub> MWCNT-PANI-RuO <sub>2</sub>	Polyaniline	Self assemble / Liquid phase	EP,tyrosine	DPV	0.16 /0.18	4.9 to 76.9	117
EB-Ppy-BSA /GCE	Polypyrrole	Self assemble / Liquid phase	EP,tyrosine	SWV	0.0074	0.1 to 400	114
Au /ZnO/Ppy/RGO	Polypyrrole	Chronoamperometry	EP, ascorbic acid, and UA	DPV	0.058	0.6 to 500	115

### 2.3 Serotonin

Poly(pyrrole-3-carboxylic acid) modified pencil graphite electrode (p(P3CA)/PGE) were electrochemically generated for serotonin sensing in biological samples<sup>122</sup>. SEM micrographs showed cauliflower-like structures of P3CA (see Figure 16) increasing the surface area in comparison with a flat surface of the bare GE. Adsorptive differential pulse stripping voltammetry was applied for determination of serotonin concentrations from 0.01  $\mu\text{M}$  to 1.0  $\mu\text{M}$  in a PBS solution at pH = 5 resulting in a LOD of 0.0025  $\mu\text{M}$ . This sensor was tested in blood serum and urine samples giving a 97.7 % to 100.6 % recovery and 93.8% to 97.4% recovery, respectively.

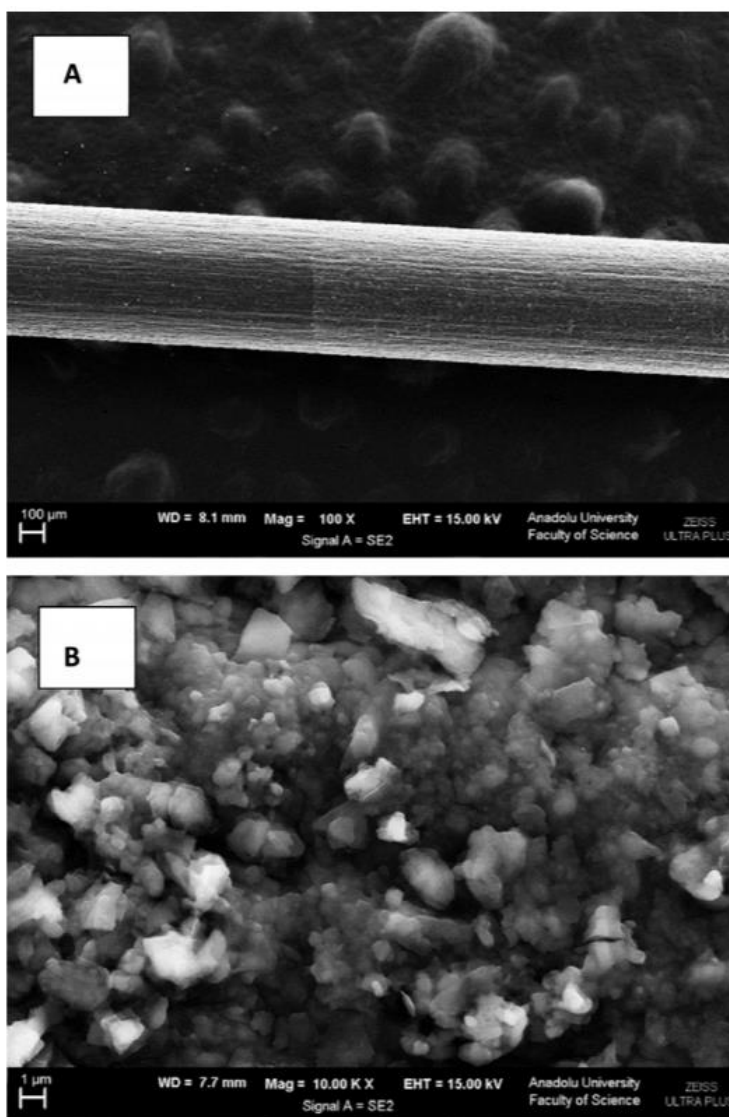


Figure 16: SEM image that allows to observe the surface of p(P3CA)/PGE in a magnification of a) 100 $\times$  and b) 10.000 $\times$  which permits to appreciate the cauliflower-like structures of P3CA. Adopted from 122

Ran et al. fabricated a poly (p-amino benzene sulfonic acid), multi-walled carbon nanotubes and chitosan nanocomposite on glassy carbon sensor (MWCNTs–CS–poly(p-ABSA) / GCE) for serotonin electrochemical detection<sup>123</sup>. Poly(p-ABSA) film was potentiodynamically obtained over GCE followed by drop casting of MWCNTs–CS suspension. DPV sensor for serotonin displayed a linear range of 0.1  $\mu\text{M}$  - 100  $\mu\text{M}$  and a detection limit of 0.080  $\mu\text{M}$  in PBS buffer solution at pH = 7, while in human blood serum was obtained a recovery between 97% and 98%. A similar monomer derivative was used for the construction of a graphene (GR) / poly 4-amino-3-hydroxy-1-naphthalenesulfonic acid modified screen printed carbon sensor (GR/p-AHNSA/SPCs) for simultaneous detection of dopamine and serotine <sup>124</sup>.FE-SEM micrographs exposed that p-AHNSA was deposited over SPC building nano-rod shape structures interconnected by GR resulting in large surface areas with high electrocatalytic activity. SWV sensor showed a LOD of 0.003  $\mu\text{M}$  in a serotonin concertation range of 0.05  $\mu\text{M}$  to 150  $\mu\text{M}$  in a PBS (pH 7.4) solution. This sensor was used for determination of serotonin in plasma and urine obtaining recovery values of 98.1% to 101.2%.

A well-known pH indicator has also been used for the fabrication of nanocomposites based on poly (bromocresol green), iron oxide nanoparticles and multiwalled carbon nanotubes ( $\text{Fe}_3\text{O}_4$ –MWCNT–poly(BCG) for the detection of serotonin <sup>125</sup>. This DPV sensor showed a LOD of 0.08  $\mu\text{M}$  with linear range of 0.5  $\mu\text{M}$  - 100.0  $\mu\text{M}$  in PBS (pH 7) solution. Human blood serum sample was used for testing this sensor which provide recovery values ca. 93%.

Reduced graphene oxide / poly(ethylene dioxythiophene)/poly(styrene sulfonic acid) /nafion (rGO–PEDOT/PSS-nafion) drop casted films were developed by Al-Graiti et al. for serotonin detection (see Figure 17) <sup>126</sup>. SEM images showed PEDOT/PSS avoid the restacking of rGO resulting in a GO–PEDOT/PSS smooth film. This sensor displayed a detection limit of 0.1  $\mu\text{M}$  and linear range of 1 to 10  $\mu\text{M}$  for serotonin by employing DVP in PBS solution at pH = 7.4. This sensor allowed the simultaneous detection of serotonin and dopamine.

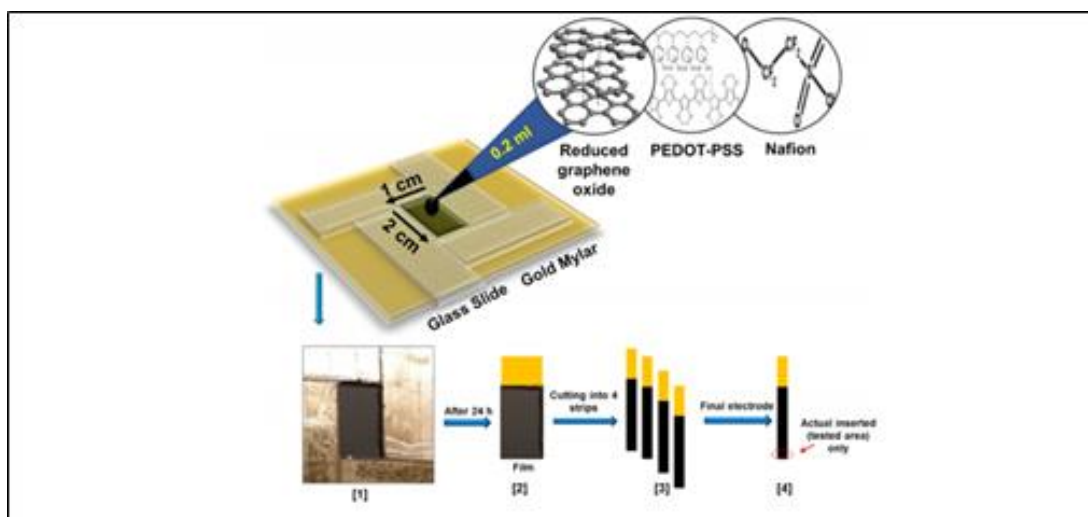


Figure 17: graphical explanation of casting process of composite onto glass slide Mylar.

Adopted from <sup>126</sup>

Chung et al. designed a dopamine and serotonin sensor based on palladium complex  $\text{Pd}(\text{C}_2\text{H}_4\text{N}_2\text{S}_2)_2$  anchored to poly2,2 :5,2-terthiophene-3-(p-benzoic acid) on AuNPs decorated reduced graphene oxide substrates ( $\text{AuNPs@rGO/pTBA-Pd}(\text{C}_2\text{H}_4\text{N}_2\text{S}_2)_2$ ) <sup>127</sup>. After drop casting AuNPs@rG onto screen printed carbon electrode, pTBA was electrodeposited over the modified working electrode by CV. Activated COOH groups allowed the immobilization of the  $\text{Pd}(\text{C}_2\text{H}_4\text{N}_2\text{S}_2)_2$  on the polymer layer by covalent bond formation. The calibration curve was made using different serotonin concentration in the range of 0.02  $\mu\text{M}$  - 20  $\mu\text{M}$  resulting in a detection limit of 0,0025  $\mu\text{M}$  by SWV in a buffer (pH 7,4) solution. This sensor was used for quantification of serotine in breast cancer cells (MCF-7) by standard addition method obtaining a recovery from 97.2% to 103.8%.

Table 3: Comparison of figures of merit conducting polymer-based sensors for the detection SER

Electrode Materials	Polymer	Synthesis Method	Analytes	Detection technique	LOD ( $\mu\text{M}$ )	Linear range ( $\mu\text{M}$ )	Ref
p(P3CA)/PGE	Poly(pyrrole-3-carboxylic acid)	CV	SER	Adsorptive differential pulse stripping voltammetry	0.0025	0.01 to 1	122
AuNPs@rGO/pTBA Pd(C <sub>2</sub> H <sub>4</sub> N <sub>2</sub> S <sub>2</sub> ) <sub>2</sub> )	poly(2,2':5,2'-terthiophene-3-(p-benzoic acid))	CV	SER and DA	SWV	0.0025	0.02 to 20	127
GR/p-AHNSA/SPCs	poly(4-amino-3-hydroxy-1-naphthalenesulfonic acid)	CV	SER and DA	SWV	0.003	0.05 to 150	124
MWCNTs-CS-poly(p-ABSA) / GCE	Poly(p-amino benzene sulfonic acid)	CV	SER	DPV	0.08	0.1 to 100	123
Fe <sub>3</sub> O <sub>4</sub> -MWCNT-poly(BCG)	poly(bromocresol green)	CV	SER	DPV	0.08	0.5 to 100	125
rGO-PEDOT/PSS	poly(ethylene dioxythiophene)/poly(styrene sulfonic acid)	Self assemble / Liquid phase	SER	DPV	0.1	1 to 10	126

## 2.4 Uric Acid

A composite of polytetraphenylporphyrin, polypyrrole, and graphene oxide (p-TPP/PPy/GO) onto glassy carbon electrode was used for detection of uric acid resulting in a LOD of 1.15  $\mu\text{M}$  with a linear range of 5  $\mu\text{M}$  - 200  $\mu\text{M}$  by DPV in PBS (pH 7) solution<sup>128</sup>. P-TPP was used for boosting the electrocatalytic activity towards oxidation of organic molecules.

$\alpha\text{-Fe}_2\text{O}_3$ /polyaniline nanotubes ( $\alpha\text{-Fe}_2\text{O}_3$ /PANI NTs) were synthesized by Mahmoudian et al. for uric acid sensing<sup>129</sup>. Polyaniline nanotubes were fabricated from a solution of acetic acid, methanol, aniline and ammonium persulfate by static synthesis for 10 hours. Then,  $\alpha\text{-Fe}_2\text{O}_3$ /polyaniline nanocomposite was assembled by stirring a solution of  $\text{FeSO}_4 \cdot 7\text{H}_2\text{O}$  and polyaniline nanotubes. TEM and FESEM allowed to confirm the formation of PAN nanotubes with presence of  $\alpha\text{-Fe}_2\text{O}_3$  spherical and hexagonal nanoparticles that increased the electrode surface area. A DPV sensor was used to build a calibration curve for uric acid concentration from 0.01  $\mu\text{M}$  to 5  $\mu\text{M}$  in PBS (pH 7) solution resulting in LOD of 0.038  $\mu\text{M}$ . Uric acid was determined in a real urine sample giving recovery values between 98.58% and 101.98%. A sensor based on functionalized polyaniline derivatives of nanostructured polyorthomethoxyaniline / multi-wall carbon nanotube onto graphite paste electrode (POMANS-MWCNT/GPE) were used for simultaneous detection of uric acid and folic acid<sup>130</sup>. A detection limit of 0.157  $\mu\text{M}$  and a linear range of 0.6  $\mu\text{M}$  - 52  $\mu\text{M}$  was determined for an LSV sensor in PBS (pH 6) solution. This electrode was tested in urine and blood serum samples given values of recovery higher than 99.6 %.

A sensitive sensor based on over-oxidized poly (3,4-ethylenedioxythiophene) nanofibers modified pencil graphite (Ox-PEDOT-nf/PGE) was developed by for uric acid detection resulting in a detection limit of 0.0013  $\mu\text{M}$  and a linear range of 0.01  $\mu\text{M}$  - 20  $\mu\text{M}$  by DPV in PBS at pH = 2<sup>131</sup>. Uric acid was sensed in urine and blood serum samples by standard addition method giving recovery values from 104% to 107%. Huang et al. synthesized poly (3,4-ethylenedioxythiophene) / graphene oxide composites on ITO electrodes (PEDOT/GO/ITO) for determination of uric acid in saliva<sup>132</sup>. Figure 18 shows the fabrication procedure for this paper-based electroanalytical device. After adding EDOT-GO suspension on ITO substrate, a potentiostatic polymerization was performed in a thin layer electrochemical cell because of its porous structure. SEM showed PEDOT-GO films as porous and rough networks. A DPV sensor displayed a LOD of 0.0013  $\mu\text{M}$  and a linear range from 2  $\mu\text{M}$  to 1000  $\mu\text{M}$  in buffer solution at pH = 6.8.

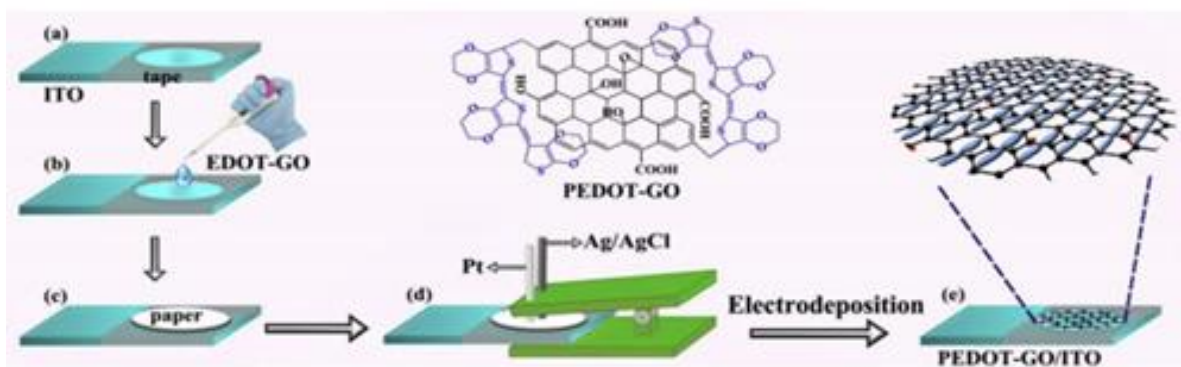
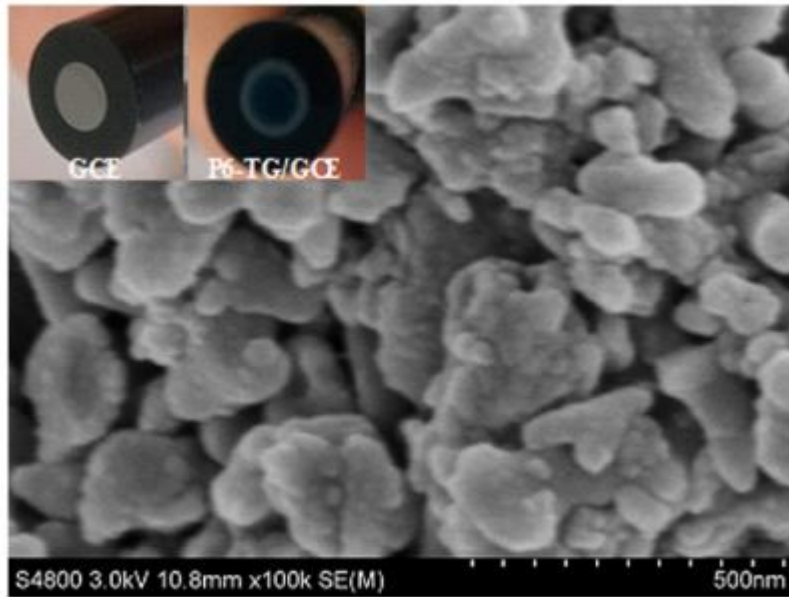


Figure 18: Graphical representation of synthesis process of Ox-PEDOT-nf/PGE . Adopted from <sup>131</sup>

Molecular imprinted poly (2-amino-5-mercapto-1, 3, 4-thiadiazole) (PAMT) and reduced graphene oxide (MIP/RGO) composite was used for simultaneous determination of uric acid and tyrosine resulting in LOD of 0.0032  $\mu\text{M}$  and a linear range from 0.01 mM to 100 mM for uric acid by DPV in PBS (pH 5) <sup>133</sup>. This sensor was tested in urine and serum showing recovery values between 94.0% and 106.0%. Poly(sulfosalicylic acid) and carboxylated graphene modified glassy carbon electrode (PSA/ERCG/GCE) sensor was employed for isoniazid and uric acid sensing <sup>134</sup>. A DPV sensor gave LOD of 0.012  $\mu\text{M}$  for a uric acid calibration curve from 0.02  $\mu\text{M}$  to 15  $\mu\text{M}$  in ammonia buffer (pH 9.0) solution. Taei et al. fabricated an Au-nanoparticles/poly-Trypan Blue modified glassy carbon electrode (AuNPs/poly-TrB /GCE) for determination of cysteine (Cys), uric acid (UA) and tyrosine (Tyr) <sup>135</sup>. After potentiodynamic deposition of polymeric film on GCE, gold nanoparticles were deposited from AuNPs suspensions by chronopotentiometry. The polymeric films appeared as an effective support for AuNp according to SEM images. A DPV sensor gave a LOD of 0.07  $\mu\text{M}$  and a linear range from 1  $\mu\text{M}$  to 550  $\mu\text{M}$  for the sensing of UA in PBS (pH 3) solution. A film of poly(6-thioguanine) on glassy carbon electrode (P6-TG/GCE) was electrogenerated by Lan and Zhang for simultaneous detection of dopamine (DA), uric acid (UA), xanthine (XA), and hypoxanthine (HXA) <sup>136</sup>. SEM images showed a rough polymeric film (see Figure 19) providing an increased effective surface area of the electrode. LOD of 0.06  $\mu\text{M}$  and a uric acid linear range from 2  $\mu\text{M}$  to 1600  $\mu\text{M}$  was determined for DVP sensor in PBS (pH 7) solution. Uric acid was determined in real samples of urine and blood serum showing recovery values >98%.



*Figure 19: Microscopy of deposited P6-TG film over glassy carbon electrode. Adopted from*

Table 4: Comparison of figures of merit conducting polymer-based sensors for the detection UA

Electrode Materials	Polymer	Synthesis Method	Analytes	Detection technique	LOD ( $\mu\text{M}$ )	Linear range ( $\mu\text{M}$ )	Ref
MIP/RGO	2-amino-5-mercapto-1, 3, 4-thiadiazole	CV	UA and tyrosine	DPV	0,0032	0.01 to 100	133
PSA/ERCG/GCE	Poly(sulfosalicylic acid)	CV	UA and isoniazid	DPV	0,012	0.02 to 15	134
Ox-PEDOT-nf/PGE	Poly (3,4 ethylenedioxythiophene)	CV	UA	DPV	0,0013	0.01 to 20	131
PEDOT/GO/ITO	Poly (3,4 ethylenedioxythiophene)	Self-assembled/liquid phase	UA	DPV	0,75	2 to 1000	132
( $\alpha$ -Fe <sub>2</sub> O <sub>3</sub> /PAN NTs	polyaniline	Self-assembled/liquid phase	UA	DPV	0,038	0.01 to 5	129
6-TG/GCE	6-thioguanine	CV	DA, UA, XA and HXA	DPV	0,06	2 to 1600	136

<b>Electrode Materials</b>	<b>Polymer</b>	<b>Synthesis Method</b>	<b>Analytes</b>	<b>Detecting technique</b>	<b>LOD (<math>\mu\text{M}</math>)</b>	<b>Linear range (<math>\mu\text{M}</math>)</b>	<b>Ref.</b>
AuNPs/poly-TrB /GCE	Au-nanoparticles/poly-Trypan Blue	CV	UA, cysteine and tyrosine	DPV	0,07	1 to 550	135
POMANS-MWCNT/GPE	Polyortho-methoxyaniline	Self-assembled/liquid phase	UA and folic acid	LSV	0,157	0.6 to 52	130
p-TPP/PPy/GO	polypyrrole	Self-assembled/liquid phase	UA	DPV	1,15	5 to 200	128

## CONCLUSIONS

This bibliography review of CP based electrochemical sensors exposed that the most used CPs for detection of dopamine, serotonin, epinephrine and uric acid are PPy, PEDOT and PANI which mainly were synthesized by potentiodynamic techniques and self-assemble techniques which required the used of initiator regent. Moreover, the detection capability of those CPs based sensor is in the order down to the nM range. These levels of detection were accomplished both using just polymer film or a composite as in the case of DA where the lowest LOD was 0.05 nM using a composite of (PPY)-Ag LSV sensor. The more sensitive methods for epinephrine detection was a sensor made of EB-Ppy-BSA /GCE with a LOD of 7.4 nM employing SWV technique. In the case of serotonin a polymeric film of Poly(pyrrole-3-carboxylic acid) deposited over GPE obtained the better result with a LOD of 2.5 nM which is the same obtained with the composite of AuNPs@rGO/pTBA Pd(C<sub>2</sub>H<sub>4</sub>N<sub>2</sub>S<sub>2</sub>)<sub>2</sub>. LOD of 1.3 nM was reported for uric acid by using an electrode of Ox-PEDOT-nf/PGE and DPV technique. An unexpected result of those review is that the most sensitive electrodes do not used DPV for its calibration curve building even when it is one of the most sensitive potentiodynamic technique.

## RECOMMENDATIONS

A research work was performed previous to development of this review. This project was about use of thin films of microporous polymer networks (MPNs) based on bi, tri and tetra carbazole monomers for detection of metronidazole, paracetamol and glyphosate. This work was stopped in the initial stages of research due to the national and international emergency by the COVID-19 pandemic. I recommend to continue with this promise project because its importance in the field of environmental chemistry because the obtained thin Films of Microporous Polymer Networks showed a great potential for detecting persistent organic contaminants in water<sup>137</sup>. Here, there is important mention that synthesis of polymer film was performed by electrochemical polymerization in a solution of monomer and support electrolyte. I consider the generation of MIP using carbazole monomer and a template is feasible to perform in order to generated a very selective sensor. Additionally, the use of surfactant must be proved for generation of different structures such as Hallowed spheres<sup>98</sup> or nano rod<sup>77</sup>. Modified Laser Scribed Graphene<sup>96</sup> appears as important option for base electrode for electropolymerization because this type of electrode is more portable than other. In other hand, there is Pencil Grafite<sup>122</sup> which showed a LOD detection limit for serotonin detection after being cover with a CP.

Additionally, the electroactive surface area of carbazole polymer films can be improved by depositing the polymer over a surface with 3D structures as Nickel Foam <sup>109</sup>and Zn nanotubes <sup>38</sup>. The use of nanoparticles, GO, carbon nanotubes and over oxidation of polymers film in a solution of NaOH must be considered as an option for solve lack of sensitivity or selectivity of sensor base on carbazole polymers.

## REFERENCES

1. K. Sinha and C. Das Mukhopadhyay, *J. Biosci.*, **45** (2020) <https://doi.org/10.1007/s12038-020-0017-x>.
2. B. Si and E. Song, *Chemosensors*, **6**, 1–24 (2018).
3. B. Si and E. Song, *Microelectron. Eng.*, **187–188**, 58–65 (2018).
4. Y. Komoto, T. Ohshiro, T. Yoshida, E. Tarusawa, T. Yagi, T. Washio, and M. Taniguchi, *Sci. Rep.*, **10**, 1–7 (2020) <https://doi.org/10.1038/s41598-020-68236-3>.
5. X. Dai, X. Fang, C. Zhang, R. Xu, and B. Xu, *J. Chromatogr. B Anal. Technol. Biomed. Life Sci.*, **857**, 287–295 (2007).
6. J. Wang, Y. Chang, W. B. Wu, P. Zhang, S. Q. Lie, and C. Z. Huang, *Talanta*, **152**, 314–320 (2016) <http://dx.doi.org/10.1016/j.talanta.2016.01.018>.
7. J. Wang, R. Du, W. Liu, L. Yao, F. Ding, P. Zou, Y. Wang, X. Wang, Q. Zhao, and H. Rao, *Sensors Actuators, B Chem.*, **290**, 125–132 (2019) <https://doi.org/10.1016/j.snb.2019.03.107>.
8. M. X. Guo and Y. F. Li, *Spectrochim. Acta - Part A Mol. Biomol. Spectrosc.*, **207**, 236–241 (2019) <https://doi.org/10.1016/j.saa.2018.09.038>.
9. A. Badoei-dalfard, N. Sohrabi, Z. Karami, and G. Sargazi, *Biosens. Bioelectron.*, **141**, 111420 (2019) <https://doi.org/10.1016/j.bios.2019.111420>.
10. N. Mohseni and M. Bahram, *Spectrochim. Acta - Part A Mol. Biomol. Spectrosc.*, **193**, 451–457 (2018) <http://dx.doi.org/10.1016/j.saa.2017.12.033>.
11. J. V. Rohit, J. N. Solanki, and S. K. Kailasa, *Sensors Actuators, B Chem.*, **200**, 219–226 (2014) <http://dx.doi.org/10.1016/j.snb.2014.04.043>.
12. Y. Zhu, Z. Yang, M. Chi, M. Li, C. Wang, and X. Lu, *Talanta*, **181**, 431–439 (2018) <https://doi.org/10.1016/j.talanta.2018.01.019>.
13. Z. Karami, N. Sohrabi, and A. Badoei-dalfard, *Biocatal. Agric. Biotechnol.*, **24**, 101549 (2020) <https://doi.org/10.1016/j.bcab.2020.101549>.
14. A. V. Bulatov, A. V. Petrova, A. B. Vishnikin, A. L. Moskvina, and L. N. Moskvina, *Talanta*, **96**, 62–67 (2012) <http://dx.doi.org/10.1016/j.talanta.2012.03.059>.
15. L. Ren, X. Hang, Z. Qin, P. Zhang, W. Wang, Y. Zhang, and L. Jiang, *Optik (Stuttg.)*, **208**, 163560 (2020) <https://doi.org/10.1016/j.ijleo.2019.163560>.
16. F. Zhang, M. Wang, D. Zeng, H. Zhang, Y. Li, and X. Su, *Anal. Chim. Acta*, **1089**, 123–130 (2019) <https://doi.org/10.1016/j.aca.2019.09.005>.
17. S. Ghosh, J. R. Bhamore, N. I. Malek, Z. V. P. Murthy, and S. K. Kailasa, *Spectrochim. Acta - Part A Mol. Biomol. Spectrosc.*, **215**, 209–217 (2019)

<https://doi.org/10.1016/j.saa.2019.02.078>.

18. J. Lv, S. Feng, Y. Ding, C. Chen, Y. Zhang, W. Lei, Q. Hao, and S. M. Chen,

*Spectrochim. Acta - Part A Mol. Biomol. Spectrosc.*, **212**, 300–307 (2019)

<https://doi.org/10.1016/j.saa.2019.01.010>.

19. F. Yan, D. Kong, Y. Luo, Q. Ye, Y. Wang, and L. Chen, *Mater. Sci. Eng. C*, **68**, 732–738

(2016) <http://dx.doi.org/10.1016/j.msec.2016.05.123>.

20. Y. Suzuki, *Sensors Actuators, B Chem.*, **239**, 383–389 (2017)

<http://dx.doi.org/10.1016/j.snb.2016.08.019>.

21. P. Sahoo, S. Das, H. S. Sarkar, K. Maiti, M. R. Uddin, and S. Mandal, *Bioorg. Chem.*, **71**,

315–324 (2017) <http://dx.doi.org/10.1016/j.bioorg.2017.03.002>.

22. D. Virág, M. Király, L. Drahos, A. E. Édes, K. Gecse, G. Bagdy, G. Juhász, I. Antal, I.

Klebovich, B. Dalmadi Kiss, and K. Ludányi, *J. Pharm. Biomed. Anal.*, **180**, 4–11 (2020).

23. E. Z. Poh, D. Hahne, J. Moretti, A. R. Harvey, M. W. Clarke, and J. Rodger, *Neurochem.*

*Int.*, **131**, 104546 (2019) <https://doi.org/10.1016/j.neuint.2019.104546>.

24. A. A. El-Sherbeni, M. R. Stocco, F. B. Wadji, and R. F. Tyndale, *J. Chromatogr. A*, **1627**

(2020).

25. C. Yilmaz, N. G. Taş, T. Kocadağlı, and V. Gökmen, *Food Chem.*, **272**, 347–353 (2019).

26. D. Wolrab, P. Frühauf, and C. Gerner, *Anal. Chim. Acta*, **937**, 168–174 (2016)

<http://dx.doi.org/10.1016/j.aca.2016.08.012>.

27. A. Rodriguez, R. M. Gomila, G. Martorell, A. Costa-Bauza, and F. Grases, *J.*

*Chromatogr. B Anal. Technol. Biomed. Life Sci.*, **1067**, 53–60 (2017)

<http://dx.doi.org/10.1016/j.jchromb.2017.09.047>.

28. W. Kwon, J. Y. Kim, S. I. Suh, and M. K. In, *Forensic Sci. Int.*, **221**, 57–64 (2012)

<http://dx.doi.org/10.1016/j.forsciint.2012.03.025>.

29. Y. Xin, Z. Li, W. Wu, B. Fu, H. Wu, and Z. Zhang, *Biosens. Bioelectron.*, **87**, 396–403

(2017) <http://dx.doi.org/10.1016/j.bios.2016.08.085>.

30. T. H. Le, J. H. Kim, and S. J. Park, *J. Cryst. Growth*, **468**, 788–791 (2017)

<http://dx.doi.org/10.1016/j.jcrysgro.2016.11.007>.

31. C. Vakh, S. Koronkiewicz, S. Kalinowski, L. Moskvina, and A. Bulatov, *Talanta*, **167**,

725–732 (2017) <http://dx.doi.org/10.1016/j.talanta.2017.02.009>.

32. W. Ding, X. Zhang, Y. L. Wu, and L. Wu, *J. Mol. Graph. Model.*, **99**, 107644 (2020)

<https://doi.org/10.1016/j.jmglm.2020.107644>.

33. X. Hun, Y. Xu, G. Xie, and X. Luo, *Sensors Actuators, B Chem.*, **209**, 596–601 (2015)

<http://dx.doi.org/10.1016/j.snb.2014.11.135>.

34. B. Huang, J. Liu, L. Lai, F. Yu, X. Ying, B. C. Ye, and Y. Li, *J. Electroanal. Chem.*, **801**, 129–134 (2017) <http://dx.doi.org/10.1016/j.jelechem.2017.07.029>.
35. R. Ramachandran, X. Leng, C. Zhao, Z. X. Xu, and F. Wang, *Appl. Mater. Today*, **18**, 100477 (2020) <https://doi.org/10.1016/j.apmt.2019.100477>.
36. N. Roy, S. Yasmin, and S. Jeon, *Microchem. J.*, **153**, 104501 (2020) <https://doi.org/10.1016/j.microc.2019.104501>.
37. N. G. Tsierkezos, U. Ritter, Y. Nugraha Thaha, A. Knauer, D. Fernandes, A. Kelarakis, and E. K. McCarthy, *Chem. Phys. Lett.*, **710**, 157–167 (2018) <https://doi.org/10.1016/j.cplett.2018.09.007>.
38. H. H. Wang, X. J. Chen, W. T. Li, W. H. Zhou, X. C. Guo, W. Y. Kang, D. X. Kou, Z. J. Zhou, Y. N. Meng, Q. W. Tian, and S. X. Wu, *Talanta*, **176**, 573–581 (2018) <http://dx.doi.org/10.1016/j.talanta.2017.08.083>.
39. Z. Lu, Y. Li, T. Liu, G. Wang, M. Sun, Y. Jiang, H. He, Y. Wang, P. Zou, X. Wang, Q. Zhao, and H. Rao, *Chem. Eng. J.*, **389**, 124417 (2020) <https://doi.org/10.1016/j.cej.2020.124417>.
40. C. Zhang, Z. Cao, G. Zhang, Y. Yan, X. Yang, J. Chang, Y. Song, Y. Jia, P. Pan, W. Mi, Z. Yang, J. Zhao, and J. Wei, *Microchem. J.*, **158**, 105237 (2020) <https://doi.org/10.1016/j.microc.2020.105237>.
41. J. Tang, Y. Liu, J. Hu, S. Zheng, X. Wang, H. Zhou, and B. Jin, *Microchem. J.*, **155**, 104759 (2020) <https://doi.org/10.1016/j.microc.2020.104759>.
42. Q. Wang, H. Si, L. Zhang, L. Li, X. Wang, and S. Wang, *Anal. Chim. Acta*, **1104**, 69–77 (2020) <https://doi.org/10.1016/j.aca.2020.01.012>.
43. M. C. Bonetto, F. F. Muñoz, V. E. Diz, N. J. Sacco, and E. Cortón, *Electrochim. Acta*, **283**, 338–348 (2018) <https://doi.org/10.1016/j.electacta.2018.06.179>.
44. Y. Yang, M. Li, and Z. Zhu, *Talanta*, **201**, 295–300 (2019) <https://doi.org/10.1016/j.talanta.2019.03.096>.
45. M. Naseri, L. Fotouhi, and A. Ehsani, *Chem. Rec.*, **18**, 599–618 (2018).
46. N. Song, Y. Wang, X. Yang, and H. Zong, *J. Electroanal. Chem.*, 114352 (2020) <https://doi.org/10.1016/j.jelechem.2020.114352>.
47. J.-M. Moon, N. Thapliyal, K. K. Hussain, R. N. Goyal, and Y.-B. Shim, *Biosens. Bioelectron.*, **102**, 540–552 (2018).
48. I. Yamaguchi, N. Fujii, and A. Wang, *React. Funct. Polym.*, **155**, 104691 (2020) <https://doi.org/10.1016/j.reactfunctpolym.2020.104691>.
49. S. Samanta, P. Roy, and P. Kar, *Mater. Sci. Eng. B Solid-State Mater. Adv. Technol.*, **256**,

- 114541 (2020) <https://doi.org/10.1016/j.mseb.2020.114541>.
50. A. J. Bard and L. R. Faulkner, *Electrochemical methods Fundamentals and Applications*, (2001).
51. N. Elgrishi, K. J. Rountree, B. D. McCarthy, E. S. Rountree, T. T. Eisenhart, and J. L. Dempsey, *J. Chem. Educ.*, **95**, 197–206 (2018).
52. C. Sandford, M. A. Edwards, K. J. Klunder, D. P. Hickey, M. Li, K. Barman, M. S. Sigman, H. S. White, and S. D. Minter, *Chem. Sci.*, **10**, 6404–6422 (2019).
53. Y. Z. Keteklahijani, (2020) <http://hdl.handle.net/1880/111491>.
54. P. Westbroek, *Anal. Electrochem. Text.*, 37–69 (2005).
55. L. G. Dias, S. G. Meirinho, A. C. A. Veloso, L. R. Rodrigues, and A. M. Peres, *Electronic tongues and aptasensors*, p. 371–402, Elsevier Ltd., (2017)  
<http://dx.doi.org/10.1016/B978-0-08-100741-9.00013-9>.
56. R. K. Franklin, S. M. Martin, T. D. Strong, and R. B. Brown, *Chemical and Biological Systems: Chemical Sensing Systems for Liquids*, p. 1–30, Elsevier Ltd., (2016)  
<http://dx.doi.org/10.1016/B978-0-12-803581-8.00549-X>.
57. A. C. and G. M. Escandar, in *Practical Three-Way Calibration*, p. 93–107 (2014).
58. A. C. Olivieri, *Chem. Rev.*, **4**, 5358–5378 (2014).
59. C. I. L. Justino, T. A. Rocha-santos, and A. C. Duarte, *Trends Anal. Chem.*, **29**, 1172–1183 (2010) <http://dx.doi.org/10.1016/j.trac.2010.07.008>.
60. F. Raposo, *TrAC - Trends Anal. Chem.*, **77**, 167–185 (2016)  
<http://dx.doi.org/10.1016/j.trac.2015.12.006>.
61. F. Bender, T. C. Chilcott, H. G. L. Coster, D. B. Hibbert, and J. J. Gooding, *Electrochim. Acta*, **52**, 2640–2648 (2007).
62. A. Palma-Cando and U. Scherf, *Macromol. Chem. Phys.*, **217**, 827–841 (2016).
63. X. X. Wang, G. F. Yu, J. Zhang, M. Yu, S. Ramakrishna, and Y. Z. Long, *Prog. Mater. Sci.*, **115**, 100704 (2021) <https://doi.org/10.1016/j.pmatsci.2020.100704>.
64. F. Ma, B. Yang, Z. Zhang, J. Kong, G. Huang, and Y. Mei, *Prog. Nat. Sci. Mater. Int.*, 0–1 (2020) <https://doi.org/10.1016/j.pnsc.2020.02.008>.
65. Y. Wang, S. Wang, L. Tao, Q. Min, J. Xiang, Q. Wang, J. Xie, Y. Yue, S. Wu, X. Li, and H. Ding, *Biosens. Bioelectron.*, **65**, 31–38 (2015)  
<http://dx.doi.org/10.1016/j.bios.2014.09.099>.
66. S. F. Kemp, R. F. Lockey, and F. E. R. Simons, *Allergy Eur. J. Allergy Clin. Immunol.*, **63**, 1061–1070 (2008).
67. Z. Soltani, K. Rasheed, D. R. Kapusta, and E. Reisin, *Curr. Hypertens. Rep.*, **15**, 175–181

(2013).

68. K. Zhou, D. Shen, X. Li, Y. Chen, L. Hou, Y. Zhang, and J. Sha, *Talanta*, **209**, 120507 (2020) <https://doi.org/10.1016/j.talanta.2019.120507>.

69. R. Jain, N. Jadon, and A. Pawaiya, *TrAC - Trends Anal. Chem.*, **97**, 363–373 (2017) <https://doi.org/10.1016/j.trac.2017.10.009>.

70. T. Qian, C. Yu, X. Zhou, S. Wu, and J. Shen, *Sensors Actuators, B Chem.*, **193**, 759–763 (2014) <http://dx.doi.org/10.1016/j.snb.2013.12.055>.

71. A. Adhikari, S. De, A. Halder, S. Pattanayak, K. Dutta, D. Mondal, D. Rana, R. Ghosh, N. K. Bera, S. Chattopadhyay, M. Chakraborty, D. Ghoshal, and D. Chattopadhyay, *Synth. Met.*, **245**, 209–222 (2018) <https://doi.org/10.1016/j.synthmet.2018.09.005>.

72. C. C. Harley, V. Annibaldi, T. Yu, and C. B. Breslin, *J. Electroanal. Chem.*, **855**, 113614 (2019) <https://doi.org/10.1016/j.jelechem.2019.113614>.

73. X. Chen, D. Li, W. Ma, T. Yang, Y. Zhang, and D. Zhang, *Microchim. Acta*, **186** (2019).

74. B. Demirkan, S. Bozkurt, K. Cellat, K. Arıkan, M. Yılmaz, A. Şavk, M. H. Çalimli, M. S. Nas, M. N. Atalar, M. H. Alma, and F. Sen, *Sci. Rep.*, **10**, 1–10 (2020).

75. Y. C. Liu, W. F. Hsu, and T. M. Wu, *J. Appl. Electrochem.*, **50**, 311–319 (2020) <https://doi.org/10.1007/s10800-019-01391-2>.

76. G. Eom, C. Oh, J. Moon, H. Kim, M. K. Kim, K. Kim, J. W. Seo, T. Kang, and H. J. Lee, *J. Electroanal. Chem.*, **848**, 113295 (2019) <https://doi.org/10.1016/j.jelechem.2019.113295>.

77. A. Adhikari, S. De, D. Rana, J. Nath, D. Ghosh, K. Dutta, S. Chakraborty, S. Chattopadhyay, M. Chakraborty, and D. Chattopadhyay, *Synth. Met.*, **260**, 116296 (2020) <https://doi.org/10.1016/j.synthmet.2020.116296>.

78. Z. Li, X. Zhou, J. Shi, X. Zou, X. Huang, and H. E. Tahir, *Food Chem.*, **276**, 291–297 (2019).

79. S. Ebrahim, A. Shokry, M. M. A. Khalil, H. Ibrahim, and M. Soliman, *Sci. Rep.*, **10**, 1–11 (2020) <https://doi.org/10.1038/s41598-020-70678-8>.

80. B. Alfano, E. Massera, A. De Maria, A. De Girolamo, G. Di Francia, P. Delli Veneri, T. Napolitano, and A. Borriello, *Proc. 2015 18th AISEM Annu. Conf. AISEM 2015*, 1–4 (2015).

81. P. M. Ashraf, K. V. Lalitha, and L. Edwin, *Sensors Actuators, B Chem.*, **208**, 369–378 (2015) <http://dx.doi.org/10.1016/j.snb.2014.10.142>.

82. S. Mahalakshmi and V. Sridevi, *Mater. Chem. Phys.*, **235**, 121728 (2019) <https://doi.org/10.1016/j.matchemphys.2019.121728>.

83. Y. H. Chang, P. M. Woi, and Y. Alias, *Microchem. J.*, **148**, 322–330 (2019) <https://doi.org/10.1016/j.microc.2019.04.081>.

84. D. Sangamithirai, S. Munusamy, V. Narayanan, and A. Stephen, *Mater. Sci. Eng. C*, **91**, 512–523 (2018) <https://doi.org/10.1016/j.msec.2018.05.070>.
85. A. A. Ganash, S. A. Alqarni, and M. A. Hussein, *J. Appl. Electrochem.*, **49**, 179–194 (2019) <http://dx.doi.org/10.1007/s10800-018-1260-9>.
86. M. M. Rahman, A. Ahmed, and J.-J. Lee, *J. Electrochem. Soc.*, **165**, B89–B95 (2018).
87. N. Dükar, S. Tunç, K. Öztürk, S. Demirci, M. Dumangöz, M. S. Çelebi, and F. Kuralay, *Mater. Chem. Phys.*, **228**, 357–362 (2019) <https://doi.org/10.1016/j.matchemphys.2019.02.043>.
88. A. Kannan and R. Sevvel, *J. Electroanal. Chem.*, **791**, 8–16 (2017) <http://dx.doi.org/10.1016/j.jelechem.2017.03.002>.
89. R. Ramkumar and M. V. Sangaranarayanan, *ChemistrySelect*, **4**, 9776–9783 (2019).
90. M. Dervisevic, M. Senel, and E. Cevik, *Mater. Sci. Eng. C*, **72**, 641–649 (2017) <http://dx.doi.org/10.1016/j.msec.2016.11.127>.
91. M. N. Gueye, A. Carella, J. Faure-Vincent, R. Demadrille, and J. P. Simonato, *Prog. Mater. Sci.*, **108**, 100616 (2020) <https://doi.org/10.1016/j.pmatsci.2019.100616>.
92. Y. Hui, C. Bian, S. Xia, J. Tong, and J. Wang, *Anal. Chim. Acta*, **1022**, 1–19 (2018) <https://doi.org/10.1016/j.aca.2018.02.080>.
93. L. Meng, A. P. F. Turner, and W. C. Mak, *Biosens. Bioelectron.*, **159**, 112181 (2020) <https://doi.org/10.1016/j.bios.2020.112181>.
94. A. L. Soares, M. L. Zamora, L. F. Marchesi, and M. Vidotti, *Electrochim. Acta*, **322**, 134773 (2019) <https://doi.org/10.1016/j.electacta.2019.134773>.
95. M. J. Donahue, A. Sanchez-Sanchez, S. Inal, J. Qu, R. M. Owens, D. Mecerreyes, G. G. Malliaras, and D. C. Martin, *Mater. Sci. Eng. R Reports*, **140**, 100546 (2020) <https://doi.org/10.1016/j.mser.2020.100546>.
96. G. Xu, Z. A. Jarjes, V. Desprez, P. A. Kilmartin, and J. Travas-Sejdic, *Biosens. Bioelectron.*, **107**, 184–191 (2018) <https://doi.org/10.1016/j.bios.2018.02.031>.
97. A. P. Sandoval-Rojas, M. T. Cortés, and J. Hurtado, *J. Electroanal. Chem.*, **837**, 200–207 (2019) <https://doi.org/10.1016/j.jelechem.2019.02.041>.
98. A. Ali, R. Jamal, T. Abdiryim, and X. Huang, *J. Electroanal. Chem.*, **787**, 110–117 (2017) <http://dx.doi.org/10.1016/j.jelechem.2017.01.051>.
99. A. Üğge, D. Koyuncu Zeybek, and B. Zeybek, *J. Electroanal. Chem.*, **813**, 134–142 (2018) <https://doi.org/10.1016/j.jelechem.2018.02.028>.
100. N. Tukimin, J. Abdullah, and Y. Sulaiman, *J. Electroanal. Chem.*, **820**, 74–81 (2018) <https://doi.org/10.1016/j.jelechem.2018.04.065>.

101. Z. Song, G. Sheng, Y. Cui, M. Li, Z. Song, C. Ding, and X. Luo, *Microchim. Acta*, **186**, 1–9 (2019).
102. Y. Qian, C. Ma, S. Zhang, J. Gao, M. Liu, K. Xie, S. Wang, K. Sun, and H. Song, *Sensors Actuators, B Chem.*, **255**, 1655–1662 (2018)  
<http://dx.doi.org/10.1016/j.snb.2017.08.174>.
103. P. Pananon, C. Sriprachuabwong, A. Wisitsoraat, P. Chuysinuan, A. Tuantranont, P. Saparpakorn, and D. Dechtrirat, *RSC Adv.*, **8**, 12724–12732 (2018)  
<http://dx.doi.org/10.1039/C8RA01564C>.
104. C. S. Inagaki, M. M. Oliveira, M. F. Bergamini, L. H. Marcolino-Junior, and A. J. G. Zarbin, *J. Electroanal. Chem.*, **840**, 208–217 (2019)  
<https://doi.org/10.1016/j.jelechem.2019.03.066>.
105. T. S. Sunil Kumar Naik, M. M. Mwaurah, and B. E. Kumara Swamy, *J. Electroanal. Chem.*, **834**, 71–78 (2019) <https://doi.org/10.1016/j.jelechem.2018.12.054>.
106. M. T. Hsieh and T. J. Whang, *J. Electroanal. Chem.*, **795**, 130–140 (2017)  
<http://dx.doi.org/10.1016/j.jelechem.2017.05.001>.
107. D. Kong, Q. Zhuang, Y. Han, L. Xu, Z. Wang, L. Jiang, J. Su, C. H. Lu, and Y. Chi, *Talanta*, **185**, 203–212 (2018) <https://doi.org/10.1016/j.talanta.2018.03.078>.
108. J. Lu, Y. Kou, X. Jiang, M. Wang, Y. Xue, B. Tian, and L. Tan, *Colloids Surfaces A Physicochem. Eng. Asp.*, **580**, 123652 (2019) <https://doi.org/10.1016/j.colsurfa.2019.123652>.
109. X. Li, X. Lu, X. Kan, X. Li, X. Lu, and X. Kan, *J. Electroanal. Chem.*, **799**, 451–458 (2017) <http://dx.doi.org/10.1016/j.jelechem.2017.06.047>.
110. N. Mohammed Modawe Alshik Edris, J. Abdullah, S. Kamaruzaman, M. I. Saiman, and Y. Sulaiman, *Arab. J. Chem.*, **11**, 1301–1312 (2018)  
<https://doi.org/10.1016/j.arabjc.2018.09.002>.
111. V. N. Palakollu and R. Karpoomath, *Synth. Met.*, **245**, 87–95 (2018)  
<https://doi.org/10.1016/j.synthmet.2018.08.012>.
112. A. Arroquia, I. Acosta, and M. P. G. Armada, *Mater. Sci. Eng. C*, **109**, 110602 (2020)  
<https://doi.org/10.1016/j.msec.2019.110602>.
113. M. T. Hsieh and T. J. Whang, *J. Electroanal. Chem.*, **795**, 130–140 (2017)  
<http://dx.doi.org/10.1016/j.jelechem.2017.05.001>.
114. R. Ramya, P. Muthukumar, and J. Wilson, *Biosens. Bioelectron.*, **108**, 53–61 (2018)  
<https://doi.org/10.1016/j.bios.2018.02.044>.
115. K. Ghanbari and A. Hajian, *J. Electroanal. Chem.*, **801**, 466–479 (2017)  
<http://dx.doi.org/10.1016/j.jelechem.2017.07.024>.

116. S. Bonyadi, K. Ghanbari, and M. Ghiyasi, *New J. Chem.*, **44**, 3412–3424 (2020).
117. T. P. Tsele, A. S. Adekunle, O. E. Fayemi, and E. E. Ebenso, *Electrochim. Acta*, **243**, 331–348 (2017) <http://dx.doi.org/10.1016/j.electacta.2017.05.031>.
118. J. Zhang, X. T. Guo, J. P. Zhou, G. Z. Liu, and S. Y. Zhang, *Mater. Sci. Eng. C*, **91**, 696–704 (2018) <https://doi.org/10.1016/j.msec.2018.06.011>.
119. F. Liu and X. Kan, *J. Electroanal. Chem.*, **836**, 182–189 (2019) <https://doi.org/10.1016/j.jelechem.2019.01.050>.
120. M. Taei, F. Hasanpour, N. Tavakkoli, and M. Bahrameian, *J. Mol. Liq.*, **211**, 353–362 (2015) <http://dx.doi.org/10.1016/j.molliq.2015.07.029>.
121. M. Ding, Y. Zhou, X. Liang, H. Zou, Z. Wang, M. Wang, and J. Ma, *J. Electroanal. Chem.*, **763**, 25–31 (2016) <http://dx.doi.org/10.1016/j.jelechem.2015.12.040>.
122. A. Özcan and S. Ilkbaş, *Sensors Actuators, B Chem.*, **215**, 518–524 (2015).
123. G. Ran, C. Chen, and C. Gu, *Microchim. Acta*, **182**, 1323–1328 (2015).
124. M. Raj, P. Gupta, R. N. Goyal, and Y. B. Shim, *Sensors Actuators, B Chem.*, **239**, 993–1002 (2017) <http://dx.doi.org/10.1016/j.snb.2016.08.083>.
125. G. Ran, X. Chen, and Y. Xia, *RSC Adv.*, **7**, 1847–1851 (2017) <http://dx.doi.org/10.1039/C6RA25639B>.
126. W. Al-Graiti, J. Foroughi, Y. Liu, and J. Chen, *ACS Omega*, **4**, 22169–22177 (2019).
127. S. Chung, M. H. Akhtar, A. Benboudiaf, D. S. Park, and Y. B. Shim, *Electroanalysis*, **32**, 520–527 (2020).
128. H. Dai, N. Wang, D. Wang, X. Zhang, H. Ma, and M. Lin, *Microchim. Acta*, **183**, 3053–3059 (2016) <http://dx.doi.org/10.1007/s00604-016-1953-x>.
129. M. R. Mahmoudian, W. J. Basirun, M. Sookhakian, P. M. Woi, E. Zalnezhad, H. Hazarkhani, and Y. Alias, *Adv. Powder Technol.*, **30**, 384–392 (2019) <https://doi.org/10.1016/j.appt.2018.11.015>.
130. H. Rajabi and M. Noroozifar, *Mater. Sci. Eng. C*, **75**, 791–797 (2017) <http://dx.doi.org/10.1016/j.msec.2017.02.133>.
131. A. Özcan and S. Ilkbaş, *Anal. Chim. Acta*, **891**, 312–320 (2015) <http://dx.doi.org/10.1016/j.aca.2015.08.015>.
132. X. Huang, W. Shi, J. Li, N. Bao, C. Yu, and H. Gu, *Anal. Chim. Acta*, **1103**, 75–83 (2020) <https://doi.org/10.1016/j.aca.2019.12.057>.
133. W. Zheng, M. Zhao, W. Liu, S. Yu, L. Niu, G. Li, H. Li, and W. Liu, *J. Electroanal. Chem.*, **813**, 75–82 (2018) <https://doi.org/10.1016/j.jelechem.2018.02.022>.
134. H. Yan, H. Xiao, Q. Xie, J. Liu, L. Sun, Y. Zhou, Y. Zhang, L. Chao, C. Chen, and S.

Yao, *Sensors Actuators, B Chem.*, **207**, 167–176 (2015)

<http://dx.doi.org/10.1016/j.snb.2014.10.002>.

135. M. Taei, F. Hasanpour, S. Habibollahi, and L. Shahidi, *Simultaneous electrochemical sensing of cysteine, uric acid and tyrosine using a novel Au-nanoparticles/poly-Trypan Blue modified glassy carbon electrode*, p. 140–147, Elsevier B.V, (2017)

<http://dx.doi.org/10.1016/j.jelechem.2017.02.035>.

136. D. Lan and L. Zhang, *J. Electroanal. Chem.*, **757**, 107–115 (2015)

<http://dx.doi.org/10.1016/j.jelechem.2015.09.018>.

137. A. Palma-Cando and U. Scherf, *ACS Appl. Mater. Interfaces*, **7**, 11127–11133 (2015).